Available online at www.sciencedirect.com
ScienceDirect
European Journal of Mechanics B/Fluids 27 (2008) 785–809

Continuum analytical modelling of thermal creep

J.G. Méolans, I.A. Graur *

Université de Provence, Ecole Polytechnique Universitaire de Marseille, UMR CNRS 6595, 5, rue Enrico Fermi, 13453 Marseille, France

Received 22 December 2006; received in revised form 25 January 2008; accepted 25 January 2008

Available online 20 February 2008

Abstract

A thermal creep process is studied in quite wide rectangular micro channels, sufficiently wide so that it is possible to consider this configuration as two parallel plates. The inlet and outlet reservoirs are maintained at the same constant pressure. A constant temperature gradient exists along the walls of the channel joining the two tanks. Thus a gas flow is induced and thermally sustained until steady conditions are reached. A complete analytical solution is derived in slip regime, yielding all the flow parameters, for Knudsen numbers smaller than 0.25. The analytical results are in good agreement with the numerical "exact" solution of the continuum equation system. Furthermore our continuum approach data are compared to those deduced from approaches based on Boltzmann equation model treatments: these various methods lead generally to a satisfactory agreement between their respective mean parameters. Nevertheless significant differences appear on the transversal velocity profiles and are further discussed.

Keywords: Rarefied flow

1. Introduction

The objective of this study is to deepen the fundamental understanding of the emerging field of microfluidic gas flows, especially in channels where tangential temperature gradients exist on the solid surfaces. As well known it is possible to generate rarefied gas flows by means of tangential temperature gradients along the channel walls: then the fluid starts creeping from the cold towards the hot regions. O.Reynolds was the first to become aware of this phenomenon and to introduce the term "thermal transpiration" in 1879. Since then, various authors have analyzed thermal creep flows by using kinetic models (BGK [1] and S-model [2]) or by solving the linearized Boltzmann equation ([3] and [4]). Thus gas velocity profiles and the mass flow rate have been numerically obtained over a large Knudsen number range. Velocity and temperature profiles have also been derived from the Navier–Stokes equations, but assuming only small compressible effects [5].

In this article we analyze the thermal creep phenomenon in rectangular micro channels sufficiently wide to consider this configuration as two parallel plates and for a fully compressible gas. We suppose that the temperature of the walls varies as a function of the x-streamwise direction and that the pressures in the tanks located at the channel inlet and

* Corresponding author.
E-mail addresses: irina.graour@polytech.univ-mrs.fr, irina_martin5@yahoo.fr (I.A. Graur).

0997-7546/$ – see front matter
doi:10.1016/j.euromechflu.2008.01.005

outlet sections are maintained equal: thus we focus our interest on the stationary flows in slip regime. The Knudsen numbers, calculated at the exit of the channel and based on the channel height, range from 0.01 to 0.25.

In Section 2 we develop the two-dimensional Cartesian NS system supplemented with slip and jump first order boundary conditions at the wall. In Section 3 we construct the tools used in our dimensional analysis. First, we choose the physical parameters and space variables in such *a way* that all the spatial derivative operators save the order of magnitude of the non-dimensional physical quantities. Then we define the corresponding dimensionless characteristic numbers governing the flows. In Section 4 we begin to simplify the non-dimensional system using a perturbation method according to a small geometric parameter. Then, in Sections 5 and 6 some realistic basic assumptions are used to simplify further the analytical system. Based on the channel geometry and also on the thermal boundary conditions (inlet/outlet temperatures) we assume that the *order of magnitude* of the transversal to longitudinal heat flux ratio is not changed by the motion of the gas. Moreover, for the same reasons, we admit that the equilibrium pressures, respectively reached in the inlet and outlet tanks, when the rest situation would occur if using small-sized tanks, would be certainly of the same order as (and rather close to) the initial reservoir pressures which are maintained constant in our real physical conditions. Thus, such conditions allow us to use, simultaneously, results derived from two different energy balances devoted to the determination of various magnitude orders, i.e. a first exclusively thermal balance for the gas at rest, and a second mechanical and thermal balance characterizing the moving gas. From both these *kinds* of evaluations we obtain the Reynolds number *order of magnitude* and we derive the reference velocity as an explicit function of the inlet/outlet pressure and temperatures. Thus, simplifications of the system are carried out in Sections 7–9. From this, velocity and pressure profiles, and heat flux are deduced in Section 10, where the mass flow rate expression is also provided. In Section 11 *are* presented the full NS numerical calculations for different micro channels sizes, wall temperature gradients, pressures and gases: a very good complete agreement with the analytical results is clearly shown. Moreover a comparison with the results obtained from kinetic methods [2] is also discussed. At last the analytical expression of mass flow rate is used to compare easily the respective properties of isothermal or thermal creep flows properties for the same mass flow rate values: we give the dimensionless pressure and/or temperature gradient respectively needed in each flow. This comparison appears useful for *conception of* the micro devices.

2. Equation system and boundary conditions

2.1. Equation system

We consider the flow in wide rectangular micro channels connecting two reservoirs maintained at the same pressure. The temperatures in the inlet and outlet reservoir are equal to T_{in} and to T_{out} respectively. We suppose that the temperature of the walls varies as a linear function of the x-streamwise direction from $T_{w_{\text{in}}}$ to $T_{w_{\text{out}}}$. Under these conditions the gas begins to flow from the cold to the hot tank. This is called the thermal creep effect. In this study we analyze this thermal creep phenomenon in channels where the value of the height H is *larger* than that of the mean free path and much smaller than that of the channel length L or width w, which means that it is possible to consider this configuration as two infinite parallel plates. According to the geometry shown in Fig. 1, the physical

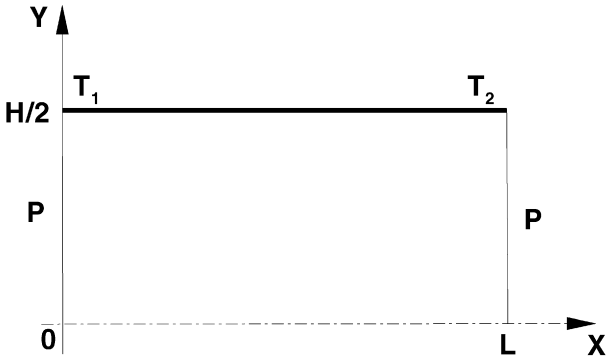

Fig. 1. A schematic diagram of the problem.

Table 1
Physical constants of the gases under standard conditions

Parameter	He	N_2	Air
viscosity (μ_{ref}) (10^{-5} Pa s)	1.865	1.656	1.709
viscosity index (ω)	0.66	0.74	0.76
specific gas constant ($\mathcal{R}$) (J kg^{-1} K^{-1})	2077.	297.	287.
$A(\omega)$	1.112	1.034	1.014
ratio of specific heats (γ)	1.67	1.4	1.4

parameters depend only on the (x, y) spatial coordinates. Then, the Navier–Stokes equations, used to describe the stationary flows, read

$$\frac{\partial \rho u}{\partial x} + \frac{\partial \rho v}{\partial y} = 0, \tag{1}$$

$$\frac{\partial \rho u^2}{\partial x} + \frac{\partial \rho uv}{\partial y} = -\frac{\partial p}{\partial x} + \frac{4}{3}\frac{\partial}{\partial x}\mu\frac{\partial u}{\partial x} - \frac{2}{3}\frac{\partial}{\partial x}\mu\frac{\partial v}{\partial y} + \frac{\partial}{\partial y}\mu\frac{\partial u}{\partial y} + \frac{\partial}{\partial y}\mu\frac{\partial v}{\partial x}, \tag{2}$$

$$\frac{\partial \rho uv}{\partial x} + \frac{\partial \rho v^2}{\partial y} = -\frac{\partial p}{\partial y} + \frac{\partial}{\partial x}\mu\frac{\partial v}{\partial x} + \frac{\partial}{\partial x}\mu\frac{\partial u}{\partial y} + \frac{4}{3}\frac{\partial}{\partial y}\mu\frac{\partial v}{\partial y} - \frac{2}{3}\frac{\partial}{\partial y}\mu\frac{\partial u}{\partial x}, \tag{3}$$

$$\begin{aligned}\frac{\partial}{\partial x}u(E+p) + \frac{\partial}{\partial y}v(E+p) = {} & \frac{4}{3}\frac{\partial}{\partial x}\mu u\frac{\partial u}{\partial x} + \frac{\partial}{\partial x}\mu v\frac{\partial v}{\partial x} - \frac{2}{3}\frac{\partial}{\partial x}\mu u\frac{\partial v}{\partial y} + \frac{\partial}{\partial x}\mu v\frac{\partial u}{\partial y} + \frac{\partial}{\partial x}\kappa\frac{\partial T}{\partial x} \\ & + \frac{\partial}{\partial y}\mu u\frac{\partial u}{\partial y} + \frac{4}{3}\frac{\partial}{\partial y}\mu v\frac{\partial v}{\partial y} + \frac{\partial}{\partial y}\mu u\frac{\partial v}{\partial x} - \frac{2}{3}\frac{\partial}{\partial y}\mu v\frac{\partial u}{\partial x} + \frac{\partial}{\partial y}\kappa\frac{\partial T}{\partial y},\end{aligned} \tag{4}$$

where the macroscopic flow quantities are noted ρ (density), u, v (velocity *components*), p (pressure) and $E = 0.5\rho(u^2 + v^2) + \rho e$ (total energy per volume unit), where μ is the viscosity coefficient, $\kappa = c_p\mu/Pr$ is the heat conductivity coefficient, Pr is the Prandtl number, $\gamma = c_p/c_v$ is the ratio of heat capacities, $e = p/(\rho(\gamma - 1))$ is the internal energy per mass unit. The gas *equation of state* involving the specific gas constant $\mathcal{R}$ is given by

$$p = \rho\mathcal{R}T. \tag{5}$$

Finally the viscosity is treated within the variable hard sphere (VHS) model, which leads to the following thermal dependence [6]:

$$\mu = \mu_{\text{ref}}\left(\frac{T}{T_{\text{ref}}}\right)^{\omega}, \tag{6}$$

where ω the viscosity index ($0.5 \leqslant \omega \leqslant 1$) depends on the type of gas and where μ_{ref} is the viscosity coefficient for the reference temperature T_{ref} (see Table 1).

2.2. Boundary conditions

The boundary conditions for the equation system (1)–(4) are the symmetry conditions on the axis and the slip velocity and the temperature jump conditions on the solid wall. Considering Knudsen number first order conditions only, the complete slip boundary condition on the upper solid wall ($y = H/2$, see Fig. 1) reads [7]

$$u_s = -\sigma_p\frac{\mu}{p}v_m\left(\frac{\partial u}{\partial y}\right)_w + \sigma_T\frac{\mu}{\rho}\left(\frac{\partial \ln T}{\partial x}\right)_w, \tag{7}$$

where $v_m = \sqrt{2\mathcal{R}T_w(x)}$ is the most probable molecular velocity at the surface temperature T_w; σ_p is the slip velocity coefficient and σ_T is the thermal slip coefficient. In this article we use the velocity slip coefficient $\sigma_p^K = 1.012$ given in [7], under the full accommodation assumption. This value, taking into account the Knudsen layer influence, is also close to the one proposed in [8] $\sigma_p^C = 1.016$. Concerning the thermal slip coefficient σ_T numerous theoretical data are summarized in [9]. Measurements of this thermal slip coefficient for various gases are carried out in [10], these

Table 2
The measured values of coefficient σ_T

Parameter	He	N_2	Air
σ_T [10]	1.004	0.923	–

measured values are given in Table 2. In the present work the well known value of σ_T, suggested in [7] and equal to 0.84, the calculated helium value from [9] ($\sigma_T = 1.175$), and also the measured air value from [10], are used.

Finally a boundary condition proposed by [7] is chosen to describe the temperature jump at the wall:

$$T_s - T_w = -\xi_T \frac{\mu}{p} v_m \left(\frac{\partial T}{\partial y}\right)_w, \tag{8}$$

where ξ_T is the temperature jump coefficient. For this coefficient, [11] and then [12] proposed a first expression of ξ_T. In this work we used the expression proposed by [7] under diffuse reflection assumption and taking into account the Knudsen layer effect, then $\xi_T = 1.173 \frac{\gamma}{4(\gamma-1)} \frac{\sqrt{\pi}}{Pr}$. Similar values of the temperature jump coefficient were obtained by [13].

Furthermore the mean free path is usually written as a function of macroscopic parameters

$$\lambda = k_\lambda \frac{\mu}{p} \sqrt{\mathcal{R}T},$$

where the coefficient k_λ depends on the molecular interaction model. A very usual choice [8] consists in retaining $k_\lambda = \sqrt{\pi/2}$, i.e. a value close to that obtained from the hard sphere model (HS) [14]. In the present study we retain $k_\lambda = A(\omega) = \frac{2(7-2\omega)(5-2\omega)}{15\sqrt{2\pi}}$, the expression used in [6] for the variable hard sphere model (VHS), more general than the HS model, where the coefficient $A(\omega)$ depends only on the type of gas (see Table 1).

3. Dimensional analysis

A steady state flow is studied now, therefore the time derivatives are not taken into account in the following analysis. The variables are *dimensionalized* in the following manner: the streamwise coordinate x by the channel length L, and the wall normal coordinate y by the channel height H. The channel height-to-length ratio ε is small compared to unit:

$$\varepsilon = H/L, \quad \varepsilon \ll 1.$$

The streamwise velocity u is normalized using the velocity u_R that is of the same order as the velocity at the channel outlet and also of the same order as the characteristic velocity of the mass flow rate (mass-flux velocity), see Section 6 for the details. Then the velocity v is normalized by εu_R. The pressure is normalized by using the pressure value at the channel exit p_{out}, where the subscript "out" refers to the outlet conditions. The temperature is normalized using the known value of the wall temperature at the channel outlet $T_{w_{\text{out}}}$; finally the density is normalized by using the appropriate outlet value $\rho_{w_{\text{out}}}$, and the viscosity coefficient by the value $\mu_{w_{\text{out}}}$ corresponding to the outlet wall temperature $T_{w_{\text{out}}}$ (according to (6)). Let us now introduce a second non-dimensional variable θ, referring to the temperature, to be used in the dimensional analysis of the equation system (1)–(4):

$$\tilde{\theta} = \frac{T - T_{\text{axe}}(x)}{T_w(x) - T_{\text{axe}}(x)}, \tag{9}$$

where T_{axe} is the temperature on the symmetry axis. As it is mentioned in the introduction, this latter form of the non-dimensional temperature has been chosen in order to obtain θ and the derivative of θ along the y-axis, both of zero order, i.e. of the same order as 1. Indeed, with this new form, it may be noticed that θ varies from zero to one along this y-axis while the non-dimensional normal coordinate y/H increases from zero to 0.5, which ensures a non-dimensional derivative mean value close to 2 (i.e. of zero order). Furthermore, in this work we consider temperature gradient driven flows where the pressure keeps, anywhere in the channel, a value close to its value p_{out} in the reservoirs. Therefore, like for the temperature and for similar reasons, we introduce a second non-dimensional variable $\tilde{\Pi}$ to represent the pressure:

$$\tilde{\Pi} = \frac{p - p_{\text{out}}}{p_M - p_{\text{out}}}, \tag{10}$$

where p_M represents the maximum pressure value in the channel. Thus choosing this $\tilde{\Pi}$ pressure form, we obtain $\tilde{\Pi}$ derivatives along the x-axis of zero order, i.e. of the same order as $\tilde{\Pi}$ itself (see Section 7). We can also relate the derivative of the $\tilde{\Pi}$ function in the x-direction with the usual form of the non-dimensional pressure

$$\frac{\partial \tilde{\Pi}}{\partial \tilde{x}} = \frac{\partial}{\partial \tilde{x}}\left(\frac{p - p_{\text{out}}}{p_M - p_{\text{out}}}\right) = \frac{1}{p_M - p_{\text{out}}}\frac{\partial p}{\partial \tilde{x}} = \frac{p_{\text{out}}}{\Delta p_M}\frac{\partial \tilde{p}}{\partial \tilde{x}} = \frac{1}{\Delta \tilde{p}_M}\frac{\partial \tilde{p}}{\partial \tilde{x}}, \tag{11}$$

and the derivative in the y-direction has the same form. Then, defining the Knudsen, Reynolds and Mach numbers based on the normalizing constant parameters retained above, we obtain:

$$Re = \frac{\rho_{w_{\text{out}}} u_R H}{\mu_{w_{\text{out}}}}, \quad Kn = \frac{\lambda}{H} = \frac{k_\lambda}{H}\frac{\mu_{w_{\text{out}}}}{p_{\text{out}}}\sqrt{\mathcal{R}T_{w_{\text{out}}}}, \quad Ma = \frac{u_R}{a_{w_{\text{out}}}}, \tag{12}$$

where $a_{w_{\text{out}}} = \sqrt{\gamma \mathcal{R} T_{w_{\text{out}}}}$ represents the velocity of the sound, based on the outlet wall temperature $T_{w_{\text{out}}}$. From the previous definitions of the non-dimensional numbers we also obtain the classical relation between Knudsen, Reynolds and Mach numbers characterizing the flow, under the form:

$$Kn = k_\lambda \sqrt{\gamma}\,\frac{Ma}{Re}. \tag{13}$$

It is necessary to remember here that we have restricted our study to the slip flow regimes characterized by a Knudsen number below 0.25. Furthermore, owing to the boundary conditions of the system, it is obvious that the flows under consideration will be low speed flows and that the typical values of their Reynolds number will be of zero order (O(1)) or of ε order (O(ε)). In addition, it is to note that practically and theoretically (in NS model) it will be consistent to neglect the Kn^2 term compared to one.

4. Equation system in non-dimensional form

The equation system (1)–(4) can be now recast into the non-dimensional following form where the expressions for Mach and Reynolds numbers (12), (13) are used and where the non-dimensional variables (introduced in Section 3) are noted with the $\sim$ symbol:

$$\frac{\partial \tilde{\rho}\tilde{u}}{\partial \tilde{x}} + \frac{\partial \tilde{\rho}\tilde{v}}{\partial \tilde{y}} = 0, \tag{14}$$

$$\frac{\partial \tilde{\rho}\tilde{u}^2}{\partial \tilde{x}} + \frac{\partial \tilde{\rho}\tilde{u}\tilde{v}}{\partial \tilde{y}} = -\frac{k_\lambda^2}{Kn^2\,Re^2}\frac{\partial \tilde{p}}{\partial \tilde{x}} + \frac{\varepsilon}{Re}\left(\frac{4}{3}\frac{\partial}{\partial \tilde{x}}\tilde{\mu}\frac{\partial \tilde{u}}{\partial \tilde{x}} - \frac{2}{3}\frac{\partial}{\partial \tilde{x}}\tilde{\mu}\frac{\partial \tilde{v}}{\partial \tilde{y}} + \frac{1}{\varepsilon^2}\frac{\partial}{\partial \tilde{y}}\tilde{\mu}\frac{\partial \tilde{u}}{\partial \tilde{y}} + \frac{\partial}{\partial \tilde{y}}\tilde{\mu}\frac{\partial \tilde{v}}{\partial \tilde{x}}\right), \tag{15}$$

$$\varepsilon^2 Kn^2 Re^2\left(\frac{\partial \tilde{\rho}\tilde{u}\tilde{v}}{\partial \tilde{x}} + \frac{\partial \tilde{\rho}\tilde{v}^2}{\partial \tilde{y}}\right) = -\frac{\partial \tilde{p}}{\partial \tilde{y}} + \varepsilon\, Kn^2 Re\left(\varepsilon^2\frac{\partial}{\partial \tilde{x}}\tilde{\mu}\frac{\partial \tilde{v}}{\partial \tilde{x}} + \frac{\partial}{\partial \tilde{x}}\tilde{\mu}\frac{\partial \tilde{u}}{\partial \tilde{y}} + \frac{4}{3}\frac{\partial}{\partial \tilde{y}}\tilde{\mu}\frac{\partial \tilde{v}}{\partial \tilde{y}} - \frac{2}{3}\frac{\partial}{\partial \tilde{y}}\tilde{\mu}\frac{\partial \tilde{u}}{\partial \tilde{x}}\right), \tag{16}$$

$$\begin{aligned}
&\frac{1}{2}\left(\frac{\partial}{\partial \tilde{x}}\tilde{\rho}\tilde{u}^3 + \varepsilon^2\frac{\partial}{\partial \tilde{x}}\tilde{\rho}\tilde{u}\tilde{v}^2 + \frac{\partial}{\partial \tilde{y}}\tilde{\rho}\tilde{u}^2\tilde{v} + \varepsilon^2\frac{\partial}{\partial \tilde{y}}\tilde{\rho}\tilde{v}^3\right) + \frac{\gamma}{\gamma - 1}\frac{k_\lambda^2}{Kn^2\,Re^2}\left(\frac{\partial \tilde{p}\tilde{u}}{\partial \tilde{x}} + \frac{\partial \tilde{p}\tilde{v}}{\partial \tilde{y}}\right)\\
&\quad = \frac{\varepsilon}{Re}\left(\frac{4}{3}\frac{\partial}{\partial \tilde{x}}\tilde{\mu}\tilde{u}\frac{\partial \tilde{u}}{\partial \tilde{x}} + \varepsilon^2\frac{\partial}{\partial \tilde{x}}\tilde{\mu}\tilde{v}\frac{\partial \tilde{v}}{\partial \tilde{x}} - \frac{2}{3}\frac{\partial}{\partial \tilde{x}}\tilde{\mu}\tilde{u}\frac{\partial \tilde{v}}{\partial \tilde{y}} + \frac{\partial}{\partial \tilde{x}}\tilde{\mu}\tilde{v}\frac{\partial \tilde{u}}{\partial \tilde{y}} + \frac{1}{\varepsilon^2}\frac{\partial}{\partial \tilde{y}}\tilde{\mu}\tilde{u}\frac{\partial \tilde{u}}{\partial \tilde{y}} + \frac{4}{3}\frac{\partial}{\partial \tilde{y}}\tilde{\mu}\tilde{v}\frac{\partial \tilde{v}}{\partial \tilde{y}}\right.\\
&\qquad \left. + \frac{\partial}{\partial \tilde{y}}\tilde{\mu}\tilde{u}\frac{\partial \tilde{v}}{\partial \tilde{x}} - \frac{2}{3}\frac{\partial}{\partial \tilde{y}}\tilde{\mu}\tilde{v}\frac{\partial \tilde{u}}{\partial \tilde{x}}\right) + \frac{\gamma}{\gamma - 1}\frac{\varepsilon k_\lambda^2}{Kn^2\,Re^3}\frac{1}{Pr}\left(\frac{\partial}{\partial \tilde{x}}\tilde{\mu}\frac{\partial \tilde{T}}{\partial \tilde{x}} + \frac{1}{\varepsilon^2}\frac{\partial}{\partial \tilde{y}}\tilde{\mu}\frac{\partial \tilde{T}}{\partial \tilde{y}}\right).
\end{aligned} \tag{17}$$

In order to eliminate the total energy E per volume unit from the energy equation (4) and obtain (17) we expressed this energy as a function of the other flow parameters: $E = 0.5\rho(u^2 + v^2) + p/(\gamma - 1)$. It is now possible to simplify the system (14)–(17).

4.1. Momentum equations

Let us start with the first momentum equation (15). Considering the amplitudes of the non-dimensional velocity variations in the $\tilde{x}$ direction (between 0 and 1) and in the $\tilde{y}$ direction (between 0 and 1/2), it is pertinent to assume (as we do) that all the non-dimensional u-velocity gradients are of zero order (i.e. of magnitude order of 1), as it is the

case for the longitudinal dimensionless velocity itself. Keeping only the respective "leaders" of the inertia forces, of the pressure forces and of the viscosity forces we obtain

$$Re\left(\frac{\partial\tilde{\rho}\tilde{u}^2}{\partial\tilde{x}}+\frac{\partial\tilde{\rho}\tilde{u}\tilde{v}}{\partial\tilde{y}}\right)=-\frac{k_\lambda^2}{Re\,Kn^2}\frac{\partial\tilde{p}}{\partial\tilde{x}}+\frac{1}{\varepsilon}\frac{\partial}{\partial\tilde{y}}\tilde{\mu}\frac{\partial\tilde{u}}{\partial\tilde{y}}. \tag{18}$$

In relation (18) we can neglect the member *of left-hand side* (of ε or 1 order according to Re) compared *with the member of the right-hand side* where the last term, of $1/\varepsilon$ order is clearly preponderant. We keep provisionally the first term expecting to discuss the magnitude order of the streamwise pressure gradient in next section:

$$\frac{\varepsilon k_\lambda^2}{Re\,Kn^2}\frac{\partial\tilde{p}}{\partial\tilde{x}}=\frac{\partial}{\partial\tilde{y}}\tilde{\mu}\frac{\partial\tilde{u}}{\partial\tilde{y}}. \tag{19}$$

Otherwise from (16) $\partial\tilde{p}/\partial\tilde{y}$ appears clearly of a *order of magnitude* smaller than (or equal to) $\varepsilon\,Kn^2$. Thus at zero order approximation equation (16) reduces to

$$\frac{\partial\tilde{p}}{\partial\tilde{y}}=0. \tag{20}$$

4.2. Energy equation

We can now simplify energy equation (17). In (17), we keep only the dominant terms in each group of terms ranging in the same brackets as it was done in (15). In the LHS of (17) the terms proportional to the ε^2 in the first brackets can be neglected. Among the terms of viscous dissipation in the RHS, the term $\frac{1}{\varepsilon^2}\frac{\partial}{\partial\tilde{y}}\tilde{\mu}\tilde{u}\frac{\partial\tilde{u}}{\partial\tilde{y}}$, inside the first brackets, is obviously dominant. For the terms describing the heat transfer, it is not possible to estimate immediately the orders of magnitude of each term, because as suggested above, in Section 3, the thermal derivative operators in the y direction do not keep the order of magnitude of the thermal variables. Therefore we cannot analyze these terms now. But we may simplify further equation (17) multiplying both the members by $\frac{\gamma-1}{\gamma}\frac{Kn^2}{k_\lambda^2}\varepsilon\,Re$ and taking into account the comments on Re and Kn^2 orders mentioned at the end of Section 3. In any way the first term of LHS is negligible compared *with* the second one. Finally it remains:

$$\frac{\varepsilon}{Re}\left(\frac{\partial\tilde{p}\tilde{u}}{\partial\tilde{x}}+\frac{\partial\tilde{p}\tilde{v}}{\partial\tilde{y}}\right)=\frac{\gamma-1}{\gamma}\frac{Kn^2}{k_\lambda^2}\frac{\partial}{\partial\tilde{y}}\tilde{\mu}\tilde{u}\frac{\partial\tilde{u}}{\partial\tilde{y}}+\frac{\varepsilon^2}{Re^2}\frac{1}{Pr}\left(\frac{\partial}{\partial\tilde{x}}\tilde{\mu}\frac{\partial\tilde{T}}{\partial\tilde{x}}+\frac{1}{\varepsilon^2}\frac{\partial}{\partial\tilde{y}}\tilde{\mu}\frac{\partial\tilde{T}}{\partial\tilde{y}}\right). \tag{21}$$

In order to simplify the analytical equation system even more, it is now necessary to consider the energy balance in the micro channel that will allow us to write a relation between the temperature difference along the wall and the exit velocity, i.e. to specify an additional relation linking the Mach and the Reynolds numbers.

5. Thermal boundary conditions and first energy balance

The sequel of the dimensional analysis of the magnitude orders in system (19)–(21) is based on energy balances. Two types of energy balance are considered in the channel:

- a first thermal balance with a gas macroscopically at rest;
- a second thermal balance with the real gas flow.

5.1. General comments on the thermal conditions

The first energy balance expresses that in the gas macroscopically in rest the transversal heat flux is globally equal to the energy loss due to the streamwise heat flux. From this first balance we can find the respective orders of transversal and longitudinal temperature differences and also the order of the corresponding dimensionless thermal parameters. Moreover, in a second energy balance, taking into account the low mass flow rates, the low Mach and Reynolds numbers under consideration, as well as the thermal boundary conditions, the thermal modifications due to the gas flow are assumed to be small: thus we can reasonably admit that the *order of magnitude* of the transversal

conductive transfer to longitudinal heat transfer ratio (per surface unit) cannot change when the flow starts. Before writing these balances the thermal conditions ensuring the present analytical modeling validity should be specified. The following developments are supported by a choice concerning the "driver" inlet/outlet temperature difference, namely:

$$T_{\text{out}} - T_{\text{in}} \sim T_{\text{in}}, \quad \text{or} \quad T_{\text{out}} \sim 2T_{\text{in}}, \tag{22}$$

where the $\sim$ symbol indicates the same order of magnitude. It is to be pointed out that in terms of magnitude order (22) is equivalent to

$$\tilde{T} \sim 1 \quad \text{and} \quad \frac{\partial \tilde{T}}{\partial \tilde{x}} \sim 1. \tag{23}$$

Correspondingly similar relations are assumed on the streamwise velocities.

5.2. First energy balance

To analyze the energy flux in the channel we assume first that the mass-flux velocity is equal to zero. It is to note that this event does not represent only a fictitious situation; as it is well known this occurs when maintaining the inlet and outlet tanks respectively to temperatures T_{in} and T_{out} (with $T_{\text{out}} > T_{\text{in}}$) and using two medium-sized tanks, perfectly closed and initially both at the same pressure: then the pressures vary in the tanks and when the induced pressure gradient exactly balances the temperature gradient effects, the gas reaches a macroscopic rest situation. Furthermore, considering the thermal boundary conditions employed here, it is obvious that the outlet and inlet pressures reached in this "rest situation" would be of same order as the pressure p_{out} maintained in the tanks in the real steady conditions; and, more generally, the *order of magnitude* of the mean thermodynamic parameters would remain the same too. Then the first energy balance indicates only that globally the transversal heat flux through the channel is counter-balanced by the energy loss owing to the longitudinal energy flux:

$$|\bar{q}_x|_{\text{in}} - \bar{q}_x|_{\text{out}}|Hw = (\bar{q}_y|_{y=H/2} - \bar{q}_y|_{y=0})2wL. \tag{24}$$

In this equation and in the following section the bars characterize the average values of the heat fluxes per surface unit: the streamwise flux is averaged over the transversal section and the transversal heat flux is averaged over the streamwise section. Referring to the energy balance equation (24), we can now estimate the temperature difference between the gas temperature at the symmetry axis of the channel and the gas temperature near the wall; then we deduce an evaluation of the transversal temperature derivative. Finally from the previous assumptions and comments, this evaluation will be considered as correct in the real conditions of the flow.

5.3. Estimation of the mean transversal conductive flux

We can rewrite the energy balance equation (24) in terms of the mean derivatives of the heat fluxes:

$$\frac{|\bar{q}_x|_{\text{in}} - \bar{q}_x|_{\text{out}}|}{L} HwL = \frac{(\bar{q}_y|_{y=H/2} - \bar{q}_y|_{y=0})}{H/2} wLH,$$

or considering the symmetry

$$\overline{\frac{\partial q_x}{\partial x}} \sim \overline{\frac{\partial q_y}{\partial y}} \sim \bar{q}_y\big|_{y=H/2}, \tag{25}$$

where the relation above may also be written as a relation between the temperature gradients, i.e. in non-dimensional form:

$$\overline{\frac{\partial}{\partial \tilde{x}} \tilde{\mu} \frac{\partial \tilde{T}}{\partial \tilde{x}}} \sim \frac{1}{\varepsilon^2} \overline{\frac{\partial}{\partial \tilde{y}} \tilde{\mu} \frac{\partial \tilde{T}}{\partial \tilde{y}}}, \tag{26}$$

where, according to (6), the non-dimensional viscosity coefficient may be expressed in the form:

$$\tilde{\mu} = \tilde{T}^{\omega}. \tag{27}$$

Let us note that the first member of Eq. (26) is of zero order. As a matter of fact, the non-dimensional $\tilde{x}$ coordinate variation from the inlet to the outlet section, in the streamwise direction is equal to 1, while the non-dimensional temperature variation along the channel is also of zero order but closer to $1/2$ than to one; moreover, according to (27), the viscosity coefficient variation along the channel is of the same order as the temperature variation and thus also rather close to $1/2$. This short analysis shows that the average value of the first member of Eq. (26) is closer to $1/4$ than to 1. Thus relation (26) may be rewritten more precisely:

$$4\overline{\frac{\partial}{\partial\tilde{x}}\tilde{\mu}\frac{\partial\tilde{T}}{\partial\tilde{x}}} \sim \frac{4}{\varepsilon^2}\overline{\frac{\partial}{\partial\tilde{y}}\tilde{\mu}\frac{\partial\tilde{T}}{\partial\tilde{y}}} \sim 1. \tag{28}$$

Using now the second non-dimensional temperature $\tilde{\theta}$, given by relation (9), the transversal temperature gradient may be rewritten as follows:

$$\frac{\partial\tilde{T}}{\partial\tilde{y}} = \frac{T_w(x) - T_{\text{axe}}(x)}{T_{w_{\text{out}}}}\frac{\partial\tilde{\theta}}{\partial\tilde{y}} = \Delta\tilde{T}(x)\frac{\partial\tilde{\theta}}{\partial\tilde{y}} \sim \Delta\tilde{T}_M\frac{\partial\tilde{\theta}}{\partial\tilde{y}}.$$

ΔT_M is the averaged temperature difference between the symmetry axis and the wall. Furthermore, from the previous equation we can also immediately derive for the mean values of the gradients

$$\overline{\frac{\partial}{\partial\tilde{y}}\tilde{\mu}\frac{\partial\tilde{T}}{\partial\tilde{y}}} = \Delta\tilde{T}(x)\overline{\frac{\partial}{\partial\tilde{y}}\tilde{\mu}\frac{\partial\tilde{\theta}}{\partial\tilde{y}}} \sim \Delta\tilde{T}_M\overline{\frac{\partial}{\partial\tilde{y}}\tilde{\mu}\frac{\partial\tilde{\theta}}{\partial\tilde{y}}}. \tag{29}$$

Since the transversal heat flux vanishes on the axis, its transversal variation (referred to the symmetry axis) represents the flux itself, we can admit that the averaged value of the $\tilde{y}$-derivative of the transversal flux is of the same order as this flux. Furthermore expressing now the transversal flux variation as a function of the second non-dimensional temperature form $\tilde{\theta}$ (as was done in the second member of (29)) we notice (as was said in Section 3) that a transversal variation of $\tilde{\theta}$ equal to 1 occurs over a non-dimensional distance axis/wall equal to $1/2$: hence the value of the dimensionless transversal flux at the wall can be estimated close to 2, and consequently the mean value of its $\tilde{y}$-derivative can be estimated as zero order and not very different from 4. Thus:

$$\overline{\frac{\partial}{\partial\tilde{y}}\tilde{\mu}\frac{\partial\tilde{T}}{\partial\tilde{y}}} \sim 4\Delta\tilde{T}_M\frac{1}{4}\overline{\frac{\partial}{\partial\tilde{y}}\tilde{\mu}\frac{\partial\tilde{\theta}}{\partial\tilde{y}}} \sim 4\Delta\tilde{T}_M\overline{\tilde{\sigma}(\tilde{x},\tilde{y})}, \tag{30}$$

where $\tilde{\sigma}(\tilde{x},\tilde{y})$ is a function of zero order and $\overline{\tilde{\sigma}(\tilde{x},\tilde{y})}$ is close to 1. Substituting the expression of the mean transversal flux variation (30) in relation (28) we obtain:

$$4\overline{\frac{\partial}{\partial\tilde{x}}\tilde{\mu}\frac{\partial\tilde{T}}{\partial\tilde{x}}} \sim \frac{16}{\varepsilon^2}\Delta\tilde{T}_M\overline{\tilde{\sigma}(\tilde{x},\tilde{y})} \sim 1. \tag{31}$$

From the previous relation we can deduce:

$$\Delta\tilde{T}_M \sim \frac{\varepsilon^2}{16}. \tag{32}$$

In addition we have now an estimation of the transversal variation of the transversal flux, i.e. an estimation of its y-derivative. *Therefore* we may consider that, at any point, the non-dimensional y-derivative of the transversal flux is of the same order as the transversal flux itself. Thus, completing relation (26) we can write:

$$\frac{\partial}{\partial\tilde{y}}\tilde{\mu}\frac{\partial\tilde{T}}{\partial\tilde{y}} \sim \tilde{\mu}\frac{\partial\tilde{T}}{\partial\tilde{y}}. \tag{33}$$

Moreover, from relations (30)–(32) we deduce

$$\frac{\partial}{\partial\tilde{y}}\tilde{\mu}\frac{\partial\tilde{T}}{\partial\tilde{y}} \sim 4\Delta\tilde{T}_M\tilde{\sigma}(\tilde{x},\tilde{y}) \sim \frac{\varepsilon^2}{4}\tilde{\sigma}(\tilde{x},\tilde{y}). \tag{34}$$

Therefore, from (33) and (34) defining precisely we can write the y-temperature derivative under the forms

$$\frac{\partial\tilde{T}}{\partial\tilde{y}} = \frac{\varepsilon^2}{4}\frac{\tilde{\sigma}(\tilde{x},\tilde{y})}{\tilde{\mu}} = \frac{\varepsilon^2}{4}\tilde{\varphi}(\tilde{x},\tilde{y})\tilde{T}(\tilde{x},\tilde{y}), \tag{35}$$

where $\tilde{\varphi}(\tilde{x},\tilde{y})$ is a new unknown function of zero order. In addition, from the thermal boundary condition on the symmetry axis, $\partial\tilde{T}/\partial\tilde{y}=0$, it is possible to conclude that $\tilde{\varphi}(\tilde{x},0)=0$.

On the basis of relation (35) it is possible to draw important conclusions concerning the zero order temperature profiles. We can write:

$$T=T(x)e^{\frac{\varepsilon^2}{4}\tilde{\psi}},\quad \tilde{\varphi}=\partial\tilde{\psi}/\partial\tilde{y},\quad \tilde{\psi}=\int_0^{\tilde{y}}\tilde{\varphi}\,dt,$$

where the zero order functions $\tilde{\varphi}$ and $\tilde{\psi}$ remain provisionally unknown. Then from the previous relations we may conclude that at zero order, and up to second order, we have $T=T(x,0)=T(x)$, and moreover $T-T(x,0)$ is of the second order according to ε, so:

$$T=T(x,0)e^{\frac{\varepsilon^2}{4}\tilde{\psi}}. \tag{36}$$

As it was mentioned in Section 2, we suppose that the temperature of the walls varies as a x-linear function in the streamwise direction from $T_{w_{\text{in}}}$ to $T_{w_{\text{out}}}$ so that, according to (36), the derivative of the temperature in the x direction equals (up to ε second order) a constant noted K_w. Thus we can write at the zero order approximation:

$$\frac{\partial\tilde{T}}{\partial\tilde{x}}=K_w,\quad \text{consequently}\quad \frac{\partial^2\tilde{T}}{\partial\tilde{x}^2}=0. \tag{37}$$

These relations will be necessary to solve the energy equation.

6. Second energy balance in the real flow

In the stationary flow regime the energy provided, per time unit, normally to the wall by the conduction is equal to the difference between the leaving energy flux (at the outlet section) and the entering energy flux (at the inlet section) where the energy quantity flowing through the 'out' and 'in' sections comprises the transported energy (macroscopic kinetic energy, internal energy, and pressure energy) supplemented with the heat flux diffused through these sections. Furthermore, from analyzing Eq. (21) we deduced which are the main quantities involved in the energy balance written over all the surfaces limiting the channel at time t. Thus it is clear that:

- the local viscous heating along x (gradient in x direction) is missing because negligible. On the other hand, the transversal viscous heating (gradient in y direction) does not globally contribute to the total energy balance, because it corresponds to an internal volumic phenomenon induced from the incoming kinetic energy and recovered through the heat flux.
- Again it is evident that in the transport terms of (21) LHS, only the derivative in x-direction $\partial\tilde{u}/\partial\tilde{x}$ contributes to the global evaluation of the leaving and the entering energies.

Thus, retaining only the dominant transport and heat flux terms corresponding to the phenomena acting in the global balance equation (21) reduces to:

$$\frac{\partial\tilde{p}\tilde{u}}{\partial\tilde{x}}\sim\frac{\varepsilon}{Re}\frac{1}{Pr}\left(\frac{\partial}{\partial\tilde{x}}\tilde{\mu}\frac{\partial\tilde{T}}{\partial\tilde{x}}+\frac{1}{\varepsilon^2}\frac{\partial}{\partial\tilde{y}}\tilde{\mu}\frac{\partial\tilde{T}}{\partial\tilde{y}}\right). \tag{38}$$

From this relation we can reach the balance equation replacing the mean value of the gradients by using the boundary value differences between the corresponding quantities:

$$\tilde{p}\tilde{u}\big|_{\text{out}}-\tilde{p}\tilde{u}\big|_{\text{in}}\sim\frac{\varepsilon}{Re}\frac{1}{Pr}\left(\left(\frac{\partial\tilde{T}}{\partial\tilde{x}}\right)_{w_{\text{out}}}-\tilde{\mu}_{w_{\text{in}}}\left(\frac{\partial\tilde{T}}{\partial\tilde{x}}\right)_{w_{\text{in}}}\right)+\frac{2}{\varepsilon Re}\frac{1}{Pr}\tilde{\mu}_w\left(\frac{\partial\tilde{T}}{\partial\tilde{y}}\right)_w. \tag{39}$$

It can be noted that the two terms in the RHS of Eq. (39) are positive and represent the contribution of the heat fluxes respectively in the streamwise and the normal direction to the wall. These two terms are of the same order, and we consider as obvious that the flow cannot change *the orders of magnitude of the various heat fluxes as evaluated at*

rest. Consequently, according to (24) we also obtain a correct relation between the magnitude orders of the various parameters if replacing the second term in RHS of Eq. (39) by the first one in which the temperatures are known, thus:

$$\tilde{p}\tilde{u}\big|_{\text{out}} - \tilde{p}\tilde{u}\big|_{\text{in}} \sim \frac{2\varepsilon}{Re}\frac{1}{Pr}\left(\left(\frac{\partial\tilde{T}}{\partial\tilde{x}}\right)_{w_{\text{out}}} - \tilde{\mu}_{w_{\text{in}}}\left(\frac{\partial\tilde{T}}{\partial\tilde{x}}\right)_{w_{\text{in}}}\right). \tag{40}$$

Remembering that the streamwise distribution of the temperature is anywhere not far from the temperature distribution at the wall, and that $\tilde{p}_{\text{out}} = \tilde{p}_{\text{in}} = 1$, Eq. (40) reads

$$\left(1 - \frac{\tilde{u}_{\text{in}}}{\tilde{u}_{\text{out}}}\right)\tilde{u}_{\text{out}} \sim (1 - \tilde{\mu}_{w_{\text{in}}})\frac{2\varepsilon}{Re\,Pr}\left(\frac{\partial\tilde{T}}{\partial\tilde{x}}\right)_{w_{\text{out}}}. \tag{41}$$

Taking into account the dependence of the viscosity from the temperature (6) and also relations (22) and (23), the first coefficients in both (41) members appear close *to one another*. Thus (41) leads to

$$\tilde{u}|_{\text{out}} \sim 2\frac{\varepsilon}{Re}\frac{1}{Pr}\left(\frac{\partial\tilde{T}}{\partial\tilde{x}}\right)_{w_{\text{out}}} \sim \frac{\varepsilon}{Re}\frac{2}{Pr}(\tilde{T}_{w_{\text{out}}} - \tilde{T}_{w_{\text{in}}}) \sim \frac{\varepsilon}{Re}\frac{1}{Pr}.$$

In the last member we have *taken* into account that $\tilde{T}_{\text{out}} = 1$ and that, according (22) and (23), $2(1 - \tilde{T}_{w_{\text{in}}}) \sim 1$. The last equation represents an estimation of outlet velocity: $u_{\text{out}_{\text{estim}}}/u_R = \varepsilon/Re/Pr$. We choose now the reference velocity u_R equal to $u_{\text{out}_{\text{estim}}}/2$, thus

$$\frac{\varepsilon}{Re\,Pr} = 2, \qquad Re = \frac{\varepsilon}{2Pr}. \tag{42}$$

Then the explicit value of u_R results immediately from (42) through (12)

$$u_R = \frac{\varepsilon}{2p_{\text{out}}}\frac{\mathcal{R}}{Pr}\mu_{w_{\text{out}}}\frac{T_{w_{\text{out}}}}{H} = \frac{1}{2p_{\text{out}}}\frac{\mathcal{R}}{Pr}\mu_{w_{\text{out}}}\frac{T_{w_{\text{out}}}}{L}. \tag{43}$$

7. First and second momentum equations

7.1. First momentum equation

In the simplified form of the first momentum equation (19) we use relation (42) between the Reynolds and Prandtl numbers:

$$-\frac{2k_\lambda^2 Pr}{Kn^2}\frac{\partial\tilde{p}}{\partial\tilde{x}} + \frac{\partial}{\partial\tilde{y}}\tilde{\mu}\frac{\partial\tilde{u}}{\partial\tilde{y}} = 0. \tag{44}$$

Accounting for property (35) when expressing the $\tilde{y}$ derivative of the viscosity coefficient $\tilde{\mu}(\tilde{T})$ (27) and remembering also (11), the previous equation yields

$$\frac{2k_\lambda^2 Pr}{Kn^2}\Delta\tilde{p}_M\frac{\partial\tilde{\Pi}}{\partial\tilde{x}} = \frac{2k_\lambda^2 Pr}{Kn^2}\frac{\partial\tilde{p}}{\partial\tilde{x}} = \tilde{\mu}\frac{\partial^2\tilde{u}}{\partial\tilde{y}^2}. \tag{45}$$

It was clear, for obvious physical reasons (equality of the pressures in the two reservoirs), that the non-dimensional derivative of the pressure $\tilde{p}$ in the $\tilde{x}$ direction cannot actually be of order 1. This fact is now confirmed, considering again Eq. (45): assuming that the problem is *solved* in the NS approach framework, as mentioned at the end of the Section 3, it is consistent and justified to neglect the terms of Kn^2 order against one in the equations. Thus, if the non-dimensional derivative of the pressure in the x direction was strictly of zero order, then, from (45), we would have finally $\partial\tilde{p}/\partial\tilde{x} = 0$ (and hence $\tilde{\mu}\frac{\partial^2\tilde{u}}{\partial\tilde{y}^2} = 0$), which would mean a constant flow or a gas at rest. Therefore the establishment of a non-trivial regime will correspond to $\partial\tilde{p}/\partial\tilde{x} \sim Kn^2$, so that both the members of (45) become of the same order: thus the viscous forces are balanced with the pressure forces.

The same conclusion may be obtained from the definition of the new $\tilde{\Pi}$ variable. As the $\tilde{\Pi}$ non-dimensional derivative in the $\tilde{x}$ direction appears clearly of zero order and its mean value equals 2: indeed, as confirmed by the calculations, we will reach $\tilde{\Pi} = 1$ (and thus, also, $\Delta\tilde{\Pi} = 1$) in a position $\tilde{x}_M$ corresponding to the maximal pressure $\tilde{p}_M$,

approximately located at the semi-length of the channel ($\Delta\tilde{x} = 0.5$). The advantage is that this formulation allows us to use only non-dimensional derivation operators preserving the order of magnitude of the non-dimensional values to which they apply. From then on, we can further examine the consequences of the previous relation in terms of mean values:

$$\frac{2k_\lambda^2 Pr}{Kn^2}\Delta\tilde{p}_M \overline{\frac{\partial\tilde{\Pi}}{\partial\tilde{x}}} \sim \overline{\tilde{\mu}\frac{\partial^2\tilde{u}}{\partial\tilde{y}^2}}.$$

As was mentioned above, the mean value of the non-dimensional derivative of the pressure $\tilde{\Pi}$ in the x direction is close to 2. In addition, a similar evaluation of the zero order second member of Eq. (45), using the ratio of the transversal dimensionless velocity increase to the dimensionless coordinate increase (and then the gradient velocity increase), yields obviously a mean value close to 4. Thus replacing in the right and left members of Eq. (45) the derivatives by their mean values, we obtain:

$$\frac{2k_\lambda^2 Pr}{Kn^2}\Delta\tilde{p}_M 2 \sim 4, \quad \text{or} \quad \Delta\tilde{p}_M \sim \frac{Kn^2}{k_\lambda^2 Pr}, \tag{46}$$

which is a pressure variation estimation perfectly consistent with a dimensionless $\tilde{p}$ gradient of Kn^2 order as determined above, i.e. $\partial\tilde{p}/\partial\tilde{x} \sim Kn^2$.

7.2. Second momentum equation

Considering then the y momentum equation (20) and replacing the pressure derivatives according to (11) we can rewrite it:

$$\frac{\partial\tilde{\Pi}}{\partial\tilde{y}} = 0 \quad \text{or} \quad \frac{\partial\tilde{p}}{\partial\tilde{y}} = 0. \tag{47}$$

8. Continuity equation

The equation of state (5) may be rewritten in the following non-dimensional form

$$\tilde{p} = \tilde{\rho}\tilde{T}. \tag{48}$$

We start the analysis of the continuity equation from the second term of Eq. (14). Replacing in this term the density by the non-dimensional expression (48) given above and using the fact that the non-dimensional form of the y-momentum equation leads to Eq. (47), we obtain:

$$\frac{\partial\tilde{\rho}\tilde{v}}{\partial\tilde{y}} = \tilde{p}\left(\frac{1}{\tilde{T}}\frac{\partial\tilde{v}}{\partial\tilde{y}} - \frac{\tilde{v}}{\tilde{T}^2}\frac{\partial\tilde{T}}{\partial\tilde{y}}\right).$$

Taking then into account relation (35) and its related comments, we can neglect the second term of ε^2 order in the right-hand side of the previous equation, and so we obtain:

$$\frac{\partial\tilde{\rho}\tilde{v}}{\partial\tilde{y}} = \frac{\tilde{p}}{\tilde{T}}\frac{\partial\tilde{v}}{\partial\tilde{y}}. \tag{49}$$

Regarding now the first term of Eq. (14) when replacing the density by the non-dimensional expression (48), we obtain:

$$\frac{\partial\tilde{\rho}\tilde{u}}{\partial\tilde{x}} = \tilde{p}\frac{\partial}{\partial\tilde{x}}\frac{\tilde{u}}{\tilde{T}} + \frac{\tilde{u}}{\tilde{T}}\frac{\partial\tilde{p}}{\partial\tilde{x}}. \tag{50}$$

For the second term in RHS of the previous equation, we use the non-dimensional pressure derivative form (11). Then using the estimation given by relation (46), the second term in the RHS of Eq. (50) appears of Kn^2 order and thus negligible against one in the NS approximation form. Therefore, Eq. (50) reduces to

$$\frac{\partial\tilde{\rho}\tilde{u}}{\partial\tilde{x}} = \tilde{p}\frac{\partial}{\partial\tilde{x}}\frac{\tilde{u}}{\tilde{T}}. \tag{51}$$

Bringing expressions (49) and (51) in the non-dimensional continuity equation (14), we eventually obtain the forms:

$$\tilde{p}\left(\frac{\partial}{\partial\tilde{x}}\frac{\tilde{u}}{\tilde{T}}+\frac{1}{\tilde{T}}\frac{\partial\tilde{v}}{\partial\tilde{y}}\right)=0,\qquad \frac{\partial\tilde{u}}{\partial\tilde{x}}+\frac{\partial\tilde{v}}{\partial\tilde{y}}=\frac{\tilde{u}}{\tilde{T}}\frac{\partial\tilde{T}}{\partial\tilde{x}}. \tag{52}$$

Thus it will be possible to eliminate the $\tilde{v}$ transversal velocity derivatives from the energy equation.

9. Energy equation

We can now continue the analysis and the simplification of the energy equation using the estimated characteristic velocity u_R to explicit the Reynolds number of the flow, like in Section 6. We rewrite the terms containing the pressure derivatives in the left-hand side of Eq. (21) using again the second non-dimensional pressure derivative (11) and replacing ε/Re by $2Pr$ according to (42). We obtain:

$$\Delta\tilde{p}_M\left(\tilde{u}\frac{\partial\tilde{\Pi}}{\partial\tilde{x}}+\tilde{v}\frac{\partial\tilde{\Pi}}{\partial\tilde{y}}\right)+\tilde{p}\left(\frac{\partial\tilde{u}}{\partial\tilde{x}}+\frac{\partial\tilde{v}}{\partial\tilde{y}}\right)=\frac{\gamma-1}{\gamma}\frac{Kn^2}{2Prk_{\lambda}^2}\frac{\partial}{\partial\tilde{y}}\tilde{\mu}\tilde{u}\frac{\partial\tilde{u}}{\partial\tilde{y}}+2\left(\frac{\partial}{\partial\tilde{x}}\tilde{\mu}\frac{\partial\tilde{T}}{\partial\tilde{x}}+\frac{1}{\varepsilon^2}\frac{\partial}{\partial\tilde{y}}\tilde{\mu}\frac{\partial\tilde{T}}{\partial\tilde{y}}\right). \tag{53}$$

As previously said, in the NS approximation we can theoretically neglect the terms of the Kn^2 order against 1: in addition we verify that this approximation is here pertinent, remembering (see Section 3) that we restricted this study to the flow regimes characterized by Knudsen numbers below 0.25, which leads to $Kn^2\leqslant 0.06$. Under this assumption the previous equation reduces to:

$$\tilde{p}\left(\frac{\partial\tilde{u}}{\partial\tilde{x}}+\frac{\partial\tilde{v}}{\partial\tilde{y}}\right)=2\left(\frac{\partial}{\partial\tilde{x}}\tilde{\mu}\frac{\partial\tilde{T}}{\partial\tilde{x}}+\frac{1}{\varepsilon^2}\frac{\partial}{\partial\tilde{y}}\tilde{\mu}\frac{\partial\tilde{T}}{\partial\tilde{y}}\right),$$

where, in the left-hand side of (53), the first term has been estimated according to (46) and thus neglected. Taking now into account Eq. (52), established in Section 8 when analyzing the continuity equation, the previous relation reads:

$$\frac{\tilde{p}\tilde{u}}{\tilde{T}}\frac{\partial\tilde{T}}{\partial\tilde{x}}=2\left(\frac{\partial}{\partial\tilde{x}}\tilde{\mu}\frac{\partial\tilde{T}}{\partial\tilde{x}}+\frac{1}{\varepsilon^2}\frac{\partial}{\partial\tilde{y}}\tilde{\mu}\frac{\partial\tilde{T}}{\partial\tilde{y}}\right). \tag{54}$$

Using Eq. (37) and the viscosity coefficient expression (27) we calculate the RHS first term in Eq. (54):

$$\frac{\partial}{\partial\tilde{x}}\tilde{\mu}\frac{\partial\tilde{T}}{\partial\tilde{x}}=\frac{\partial\tilde{\mu}}{\partial\tilde{x}}K_w=K_w^2\omega T^{\omega-1}. \tag{55}$$

Then, from relation (35) we find the temperature derivative according to y and we can calculate the RHS second term of Eq. (54), i.e. at second order:

$$\frac{1}{\varepsilon^2}\frac{\partial}{\partial\tilde{y}}\tilde{\mu}\frac{\partial\tilde{T}}{\partial\tilde{y}}\sim\frac{1}{4}\frac{\partial}{\partial\tilde{y}}(\tilde{\mu}\tilde{\varphi}\tilde{T})=\frac{1}{4}\left(\tilde{T}^{\omega+1}\frac{\partial\tilde{\varphi}}{\partial\tilde{y}}+\frac{\varepsilon^2}{4}(\omega+1)\tilde{\varphi}^2\tilde{T}^{\omega+1}\right)=\frac{\tilde{T}^{\omega+1}}{4}\frac{\partial\tilde{\varphi}}{\partial\tilde{y}}. \tag{56}$$

Taking into account the previous expressions (55) and (56), Eq. (54) reads:

$$\tilde{u}=\frac{2\tilde{T}^{\omega}}{\tilde{p}K_w}\left(\omega K_w^2+\frac{\tilde{T}^2}{4}\frac{\partial\tilde{\varphi}}{\partial\tilde{y}}\right), \tag{57}$$

and we obtain a streamwise velocity expression, depending on the unknown function $\tilde{\varphi}$, from which the velocity on the wall (slip velocity) may also be deduced. We will use this last equation in Section 10 in order to obtain the heat flux expression.

10. Velocity and pressure profiles, and heat flux expression

10.1. Velocity and pressure profiles

We now integrate the reduced form of the first momentum equation (45) in order to obtain the streamwise velocity. As previously seen (see Sections 7 and 9), $\tilde{p}$ and $\tilde{T}$ are independent of $\tilde{y}$ at zero order. Thus by integrating the two members of (45) and taking into account the boundary conditions on the symmetry axis, we obtain:

$$\frac{\partial \tilde{u}}{\partial \tilde{y}} = \frac{2k_\lambda^2 Pr}{Kn^2}\frac{1}{\tilde{T}^\omega}\frac{\partial \tilde{p}}{\partial \tilde{x}}\tilde{y}, \tag{58}$$

while integrating once again

$$\tilde{u}(\tilde{y}) = \frac{k_\lambda^2 Pr}{Kn^2}\frac{1}{\tilde{T}^\omega}\frac{\partial \tilde{p}}{\partial \tilde{x}}\left(\tilde{y}^2 - \frac{1}{4}\right) + u_s(\tilde{x}). \tag{59}$$

For the slip velocity we use the Kogan formulation [7] (7). In the non-dimensional form Eq. (7) gives

$$\tilde{u}_s = \frac{\sqrt{2}\tilde{\mu}}{\tilde{p}}\left(-\sigma_p \frac{Kn}{k_\lambda}\sqrt{\tilde{T}}\left(\frac{\partial \tilde{u}}{\partial \tilde{y}}\right)_w + \sigma_T \sqrt{2}\, Pr \tilde{T}\left(\frac{1}{\tilde{T}}\frac{\partial \tilde{T}}{\partial \tilde{x}}\right)_w\right). \tag{60}$$

From (58) we find

$$\left(\frac{\partial \tilde{u}}{\partial \tilde{y}}\right)_w = \left.\frac{\partial \tilde{u}}{\partial \tilde{y}}\right|_{\tilde{y}=0.5} = \frac{k_\lambda^2 Pr}{Kn^2}\frac{1}{\tilde{T}^\omega}\frac{\partial \tilde{p}}{\partial \tilde{x}}. \tag{61}$$

As mentioned above the temperature of the wall varies as a linear function of the streamwise direction from $T_{w_{\text{in}}}$ to $T_{w_{\text{out}}}$, so that the temperature is close to a linear function of x (at ε second order), and the derivative of the temperature along the x-direction is equal to a constant K_w (37). Using this notation K_w for the derivation of the temperature, we may write:

$$\left(\frac{1}{\tilde{T}}\frac{\partial \tilde{T}}{\partial \tilde{x}}\right)_w = \left.\frac{1}{\tilde{T}}\frac{\partial \tilde{T}}{\partial \tilde{x}}\right|_{\tilde{y}=0.5} = \frac{K_w}{\tilde{T}(x)}. \tag{62}$$

Involving relations (61) and (62) in (60) and using the non-dimensional expression for the viscosity coefficient (27) we obtain:

$$\tilde{u}_s = \frac{\sqrt{2}\, Pr}{\tilde{p}}\tilde{T}^\omega\left(-\sigma_p \frac{k_\lambda}{Kn}\frac{\sqrt{\tilde{T}}}{\tilde{T}^\omega}\left(\frac{\partial \tilde{p}}{\partial \tilde{x}}\right)_w + \sigma_T \sqrt{2}\, K_w\right). \tag{63}$$

Let us express the non-dimensional velocity profile using (59) and (63):

$$\tilde{u}(\tilde{y}) = \frac{k_\lambda^2 Pr}{4\, Kn^2}\frac{1}{\tilde{T}^\omega}\frac{\partial \tilde{p}}{\partial \tilde{x}}(4\tilde{y}^2 - 1) - \sqrt{2}\sigma_p \frac{1}{\tilde{p}}\frac{k_\lambda Pr}{Kn}\sqrt{\tilde{T}}\frac{\partial \tilde{p}}{\partial \tilde{x}} + 2\sigma_T \frac{1}{\tilde{p}} K_w Pr \tilde{T}^\omega. \tag{64}$$

In this expression of the velocity profile, the pressure distribution along the channel remains an unknown quantity and so does the pressure derivative in the x direction. In order to find these unknown distributions we start carrying out the calculation of the mass flow rate in the channel. The non-dimensional mass flow rate may be expressed as

$$\tilde{Q} = 2\int_0^{0.5} \tilde{\rho}\tilde{u}(\tilde{y})\, d\tilde{y}.$$

Substituting the expression for the velocity profile (64) in the previous relation and using the equation of state (48) we obtain

$$\tilde{Q} = -\frac{k_\lambda^2 Pr}{6\, Kn^2}\frac{\tilde{p}}{\tilde{T}^{\omega+1}}\frac{\partial \tilde{p}}{\partial \tilde{x}} - \sqrt{2}\sigma_p \frac{k_\lambda Pr}{Kn}\frac{1}{\sqrt{\tilde{T}}}\frac{\partial \tilde{p}}{\partial \tilde{x}} + 2\sigma_T K_w Pr \tilde{T}^{\omega-1}. \tag{65}$$

Now we can express the non-dimensional pressure using the definition of the second non-dimensional pressure (10) and the estimation (46) of the maximal pressure in the channel

$$\tilde{p} = 1 + \frac{p - p_{\text{out}}}{p_{\text{out}}} = 1 + \Delta\tilde{p}_M \tilde{\Pi}(\tilde{x}) = 1 + \frac{Kn^2}{k_\lambda^2 Pr}\tilde{\Pi}(\tilde{x}), \tag{66}$$

or for the derivations according to (11)

$$\frac{\partial \tilde{p}}{\partial \tilde{x}} = \frac{Kn^2}{k_\lambda^2 Pr}\frac{\partial \tilde{\Pi}(\tilde{x})}{\partial \tilde{x}}. \tag{67}$$

Replacing the non-dimensional pressure and pressure gradient in (65) we obtain

$$\tilde{Q} = -\left(1 + \frac{Kn^2}{k_\lambda^2 Pr}\tilde{\Pi}\right)\frac{1}{6\tilde{T}^{\omega+1}}\frac{\partial\tilde{\Pi}}{\partial\tilde{x}} - \sqrt{2}\sigma_p\frac{1}{\sqrt{\tilde{T}}}\frac{Kn}{k_\lambda}\frac{\partial\tilde{\Pi}}{\partial\tilde{x}} + 2\sigma_T K_w Pr\,\tilde{T}^{\omega-1}.$$

It is again to be noticed that $\tilde{\Pi}(\tilde{x})$ and $\frac{\partial\tilde{\Pi}}{\partial\tilde{x}}$ are of zero order in ε and in Knudsen number. We cannot utilize directly the obtained equation in order to find the pressure because of the presence of the *Kn* second order terms which are not significant at our approximation level. Neglecting these terms of *second order* in *Kn*, the previous equation yields

$$\tilde{Q} = -\frac{1}{6\tilde{T}^{\omega+1}}\frac{\partial\tilde{\Pi}}{\partial\tilde{x}} - \sqrt{2}\sigma_p\frac{1}{\sqrt{\tilde{T}}}\frac{Kn}{k_\lambda}\frac{\partial\tilde{\Pi}}{\partial\tilde{x}} + 2\sigma_T K_w Pr\,\tilde{T}^{\omega-1}.$$

Expressing the non-dimensional pressure derivative, it reads

$$\frac{\partial\tilde{\Pi}}{\partial\tilde{x}} = -\frac{6\tilde{T}^{\omega}(\tilde{T}\tilde{Q} - 2\sigma_T K_w Pr\,\tilde{T}^{\omega})}{1 + 6K_{\text{slip}}Kn\,\tilde{T}^{\omega+0.5}}, \quad \text{where } K_{\text{slip}} = \sigma_p\frac{\sqrt{2}}{k_\lambda}. \tag{68}$$

This equation gives the pressure gradient and makes it possible to determine the velocity profile. Putting the pressure derivative (68) equal to zero, we also find the abscise $\tilde{x}_M$ corresponding to the maximum pressure as the solution of the equation

$$\tilde{Q} = 2\sigma_T K_w Pr\tilde{T}^{\omega-1}(\tilde{x}_M).$$

This *abscise* allows us to determine the value of the maximum pressure p_M from the pressure profile that we will deduce below. From Eq. (64) we can draw the velocity profile using the expression of the $\tilde{\Pi}$ derivative (68) and the relation between first and second pressure form derivatives (67). Let us note that the pressure appears in the denominator in Eq. (64). But when replacing this pressure by the last member of (66), in which we have neglected the term of order 2 in *Kn*, $\tilde{p}$ reduces to one and we obtain

$$\tilde{u}(\tilde{y}) = \left(\frac{3}{2}(4\tilde{y}^2 - 1) - 6\,Kn_*\,\tilde{T}^{\omega+0.5}\right)\frac{2\sigma_T K_w Pr\,\tilde{T}^{\omega} - \tilde{T}\tilde{Q}}{1 + 6\,Kn_*\,\tilde{T}^{\omega+0.5}} + 2\sigma_T Pr\,K_w\tilde{T}^{\omega}, \tag{69}$$

where we use the following notation

$$Kn_* = K_{\text{slip}}\,Kn.$$

In order to deduce the pressure profile we present the pressure derivation (68) in the following form

$$\frac{\partial\tilde{\Pi}}{\partial\tilde{x}} = \frac{12\sigma_T K_w Pr\,\tilde{T}^{2\omega}}{1 + 6\,Kn_*\,\tilde{T}^{\omega+0.5}} - \frac{6\tilde{T}^{\omega+1}}{1 + 6\,Kn_*\tilde{T}^{\omega+0.5}}\tilde{Q} = A - B\,\tilde{Q}. \tag{70}$$

In order to obtain the expression for the pressure distribution along the x axis we integrate the pressure derivative (70) from 0 to $\tilde{x}$:

$$\tilde{\Pi} = \int_0^{\tilde{x}} A\,d\tilde{x} - \tilde{Q}\int_0^{\tilde{x}} B\,d\tilde{x} = \tilde{\Pi}_A - \tilde{Q}\tilde{\Pi}_B. \tag{71}$$

We start the integration with the first term which is presented in the form

$$\tilde{\Pi}_A = \int_0^{\tilde{x}} A\,d\tilde{x} = \frac{12\sigma_T Pr}{Kn_*}\int_0^{\tilde{x}} \frac{Kn_*\,\tilde{T}^{\omega+0.5}\tilde{T}^{\omega-0.5}K_w}{1 + 6\,Kn_*\,\tilde{T}^{\omega+0.5}}\,d\tilde{x}.$$

Using the relation $K_w\,d\tilde{x} = d\tilde{T}$ we finally obtain

$$\tilde{\Pi}_A = \frac{2\sigma_T Pr}{Kn_*}\left(D_{\omega+0.5}(\tilde{x}) + \frac{1}{6Kn_*(\omega+0.5)}\ln\frac{1 + 6\,Kn_*\tilde{T}_{w_{\text{in}}}^{\omega+0.5}}{1 + 6\,Kn_*\tilde{T}^{\omega+0.5}}\right), \tag{72}$$

where we use D_υ defined as

$$D_\upsilon(\tilde{x}) = \frac{\tilde{T}^\upsilon(\tilde{x}) - \tilde{T}^\upsilon_{w_{\text{in}}}}{\upsilon}.$$

For the second term of (71) we have:

$$\tilde{\Pi}_B = \int_0^{\tilde{x}} B\, d\tilde{x} = 6 \int_0^{\tilde{x}} \frac{\tilde{T}^{\omega+1}}{1 + 6\,Kn_*\,\tilde{T}^{\omega+0.5}}\, d\tilde{x}. \tag{73}$$

We can transform the fraction denominator under the integral sign in the following way:

$$1 + 6\,Kn_*\,\tilde{T}^{\omega+0.5} = (1 + 3\,Kn_*)\big(1 + c\,Kn_*(\tilde{T}^{\omega+0.5} - 0.5)\big), \tag{74}$$

where we denote the zero order coefficient

$$c = \frac{6}{1 + 3\,Kn_*}.$$

Using then relation (74), expression (73) reads

$$\tilde{\Pi}_B = \frac{c}{K_w} \int_0^{\tilde{x}} \frac{\tilde{T}^{\omega+1} K_w}{1 + c\,Kn_*\,(\tilde{T}^{\omega+0.5} - 0.5)}\, d\tilde{x}.$$

The fraction under the integral sign can now be appropriately expanded according to the Knudsen number up to the second power. Integrating this expansion from 0 to $\tilde{x}$ we obtain

$$\tilde{\Pi}_B = \frac{c}{K_w}\left(\left(1 + \frac{1}{2}c\,Kn_* + \frac{1}{4}c^2\,Kn_*^2\right) D_{\omega+2}(\tilde{x}) - c\,Kn_*(1 + c\,Kn_*)\,D_{2\omega+2.5}(\tilde{x}) + c^2\,Kn_*^2\,D_{3\omega+3}(\tilde{x})\right). \tag{75}$$

The local $\tilde{\Pi}$ expression (71) gives the mass flow rate closing the equation system: according to its definition (10), $\tilde{\Pi}$ vanishes when $\tilde{x} = 1$, therefore Eq. (71) leads to

$$\tilde{Q} = \frac{\tilde{\Pi}_A}{\tilde{\Pi}_B}\bigg|_{\tilde{x}=1}.$$

For $\tilde{x} = 1$, using the fact that the non-dimensional temperature $\tilde{T}_{w_{\text{out}}}$ is equal to 1, we obtain accounting for (72) and (75)

$$\begin{aligned}\tilde{Q} = {} & \frac{2\sigma_T\,Pr}{Kn_*}\left(D_{\omega+0.5} + \frac{1}{6\,Kn_*(\omega + 0.5)} \ln\frac{1 + 6\,Kn_*\tilde{T}^{\omega+0.5}_{w_{\text{in}}}}{1 + 6\,Kn_*}\right) \\ & \times \left[\frac{c}{K_w}\left(\left(1 + \frac{1}{2}c\,Kn_* + \frac{1}{4}c^2\,Kn_*^2\right) D_{\omega+2} - c\,Kn_*\,(1 + c\,Kn_*)\,D_{2\omega+2.5} + c^2\,Kn_*^2\,D_{3\omega+3}\right)\right]^{-1},\end{aligned} \tag{76}$$

where $D_\upsilon(\tilde{x})|_{\tilde{x}=1} = D_\upsilon$. Finally the mass flow rate expression (76) provides an explicit velocity profile from (69) and an explicit pressure distribution from (71).

In addition we can also write the dimensional mass flow rate expression

$$Q = \frac{\mu_{\text{out}} H}{4PrL}\,\tilde{Q}. \tag{77}$$

10.2. Expression of the heat transfer

Now we can find the values of the heat flux in the transversal direction from relation (35). Integrating the velocity profile given by relation (57) from 0 to $\tilde{y}$, we obtain

$$\int_0^{\tilde{y}} \tilde{u}\, d\tilde{y} = \frac{2\tilde{T}^\omega}{\tilde{p}\,K_w}\left(\omega K_w^2\,\tilde{y} + \frac{\tilde{T}^2}{4}\tilde{\varphi}(\tilde{x}, \tilde{y})\right). \tag{78}$$

Furthermore, we can use the velocity profile (69) rewritten in the form

$$u(\tilde{y}) = \left(\frac{3}{2}(4\tilde{y}^2 - 1) - 6\,Kn_*\,\tilde{T}^{\omega+0.5}\right)S + 2\sigma_T K_w\,Pr\,\tilde{T}^{\omega}, \tag{79}$$

where we use the notation S defined as

$$S = \frac{2\sigma_T K_w\,Pr\,\tilde{T}^{\omega} - \tilde{T}\,\tilde{Q}}{1 + 6\,Kn_*\,\tilde{T}^{\omega+0.5}}.$$

Integrating again the velocity profile (79) from 0 and $\tilde{y}$ we obtain

$$\int_0^{\tilde{y}} \tilde{u}\,d\tilde{y} = 2\tilde{y}^3 S + \tilde{y}\big(2\sigma_T K_w\,Pr\,\tilde{T}^{\omega} - (1.5 + 6\,Kn_*\,\tilde{T}^{\omega+0.5})S\big). \tag{80}$$

Now we can equate Eq. (80) to Eq. (78) where $\tilde{p}$ is approximated by 1, neglecting the second power in Kn (cf. (78)). We express from this the product $\tilde{\varphi}\tilde{T}$ and using relation (35) we obtain the expression for the temperature transversal derivative:

$$\frac{\partial\tilde{T}}{\partial\tilde{y}} = \varepsilon^2\frac{\tilde{T}}{4}\varphi(\tilde{x},\tilde{y}) = \varepsilon^2\frac{K_w}{\tilde{T}}\left(\frac{\tilde{y}^3 S}{\tilde{T}^{\omega}} - \tilde{y}\left(\frac{3}{4}\frac{S}{\tilde{T}^{\omega}} + 3Kn_*\tilde{T}^{0.5}S + \omega K_w - \sigma_T\,Pr\,K_w\right)\right). \tag{81}$$

Thus, in the thermal transpiration problem, where the temperature gradient $\partial\tilde{T}/\partial\tilde{x}$ is uniform, the transversal heat flux, opposite to the temperature gradient $\partial\tilde{T}/\partial\tilde{y}$ direction, is non-uniform over the section of the channel. This property of the transversal heat flux was emphasized also in [3].

From (81) we can obtain the energy flux to be furnished to the *microsystem*, per width unit, in order to maintain the stationary micro flow.

11. Numerical simulation and comparison with the analytical approach and other theories

11.1. Numerical modeling

For the numerical simulation of the micro channel flows the NS equation system (1)–(4) is solved. The computations are carried out for a two dimensional flow between the symmetry axis and the parallel plate at the distance $H/2$ (see Fig. 1). The flow is sustained by a temperature gradient. The total pressure and temperature are fixed in the inlet and outlet reservoirs. It should be remembered that the pressures are the same in both reservoirs and that the temperatures are different. The other flow parameters at the inlet and outlet sections of the channel are deduced from the characteristic equations. The basic grid used in the calculations is (131×22) cells. The calculations with the finer grid (261×42) are limited to a few cases to check whether the results are independent of the grid.

The computations are performed for different gases: helium, nitrogen and air. The main parameters of the gases are presented in the Table 1. The calculations are carried out for the channel of H of 10 μm in height and L of 1 cm in length. We have compared the analytical and numerical profiles of the flow parameters in the channel under three different types of flow conditions:

- The pressure in both tanks is equal to the atmospheric pressure $p_{\text{atm}} = 1.013 \times 10^5$ Pa, the temperature in the inlet tank is equal to 295.6 K, the temperature difference between the tanks is equal to 277.4 K. The flows of helium and of air are considered (see Table 3).
- The pressure in both tanks is equal to the atmospheric pressure p_{atm}, the temperature in the inlet tank is equal to 295 K. The different values of the temperature difference between the tanks are considered (see Table 4) and its influence on the flow is studied. The flow of nitrogen is considered.
- The temperature in the inlet tank is equal to 295 K. Different values of the pressure (the same in the two tanks) are considered (see Table 5), which correspond to different values of the Knudsen number. The influence of the Knudsen number on the flow is studied. The flow of nitrogen is considered.

Table 3
Mass flow rate calculated by: present NS numerical approach (NS (num. sol.)), present analytical approach (76) (NS (anal. sol.)), numerical solution of the Boltzmann equation (BE (S-model) [2]). The temperature difference between the inlet and outlet sections of the channel is equal to 277.4 K, the inlet and outlet pressures are equal to the atmospheric pressure, σ_T is taken equal to 0.923 for an air [10] flow and 1.175 for a helium flow [9]

Gas	He	Air
Kn_{out}	0.036	0.012
Mass flow rate (10^{-12} kg/s) NS (num. sol.)	3.767	2.842
Mass flow rate (10^{-12} kg/s) NS (anal. sol.)	3.766	2.843
Mass flow rate (10^{-12} kg/s) BE (S-model) [2]	3.458	2.844

Table 4
Mass flow rate of nitrogen flow calculated using: present NS numerical approach (NS (num.sol.)), present analytical approach (76) (NS (anal.sol.)), numerical solution of the Boltzmann equation (BE (S-model) [2]). The inlet and outlet pressures are equal to the atmospheric pressure, the temperature in the inlet reservoir is equal to 295 K, $\sigma_T = 0.923$ [10]

$T_{\text{out}} - T_{\text{in}}$ (K)	140	300	600
Kn_{out}	0.008	0.0126	0.0209
Mass flow rate (10^{-12} kg/s) NS (num.sol.)	1.449	2.929	5.371
Mass flow rate (10^{-12} kg/s) NS (anal.sol.)	1.449	2.929	5.371
Mass flow rate (10^{-12} kg/s) BE (S-model) [2]	1.449	2.929	5.596

Table 5
Mass flow rate of nitrogen flow calculated using: present NS numerical approach (NS (num.sol.)), present analytical approach (76) (NS (anal.sol.)), numerical solution of the Boltzmann equation (BE (S-model) [2]). The temperature difference between the inlet and outlet sections is equal to 300 K, $\sigma_T = 0.923$ [10]

p_{out}	p_{atm}	$0.1\,p_{\text{atm}}$	$0.05\,p_{\text{atm}}$
Kn_{out}	0.0126	0.126	0.253
Mass flow rate (10^{-12} kg/s) NS (num.sol.)	2.929	2.940	2.943
Mass flow rate (10^{-12} kg/s) NS (anal.sol.)	2.929	2.910	2.851
Mass flow rate (10^{-12} kg/s) BE (S-model) [2]	2.929	2.927	2.404

11.2. Comparisons and comments

The classical thermal transpiration phenomenon considered in many articles consists in the apparition and the development of an unsteady flow between two reservoirs. At the beginning of the experiment both reservoirs are kept at the same pressure and at different temperatures, while the temperature difference is maintained during the experiment. If these two reservoirs are connected with a micro channel the gas starts to creep from the cold to the hot reservoir until to the establishment of a well known relation between the pressures and temperatures, corresponding to a system in which the mass flow rate in the channel completely vanishes. In our investigation the temperature difference between the two reservoirs is maintained, while the pressures are kept *constant with time*. As *a result*, we obtain a steady flow from the cold to the hot reservoir. A non-linear pressure profile forms along the channel and the mass flow rate does not vanish.

Three different approaches were developed on the basis of the kinetic theory in order to model similar problems. We will give their brief description. The authors of [3] investigated the steady flow between parallel plates using the Boltzmann equation for the hard-sphere molecules, linearized around an uniform equilibrium state at rest, and the diffuse reflection condition on the wall. In addition, they assumed that the pressure gradient in the gas and the temperature gradients of the plates were small and uniform. So, a both gradients were supposed known along the plates. Contrarily in the case under consideration only the temperature gradient is known *a priori*, but not the pressure gradient, so it is impossible to use *the results of* [3] directly *for comparison*.

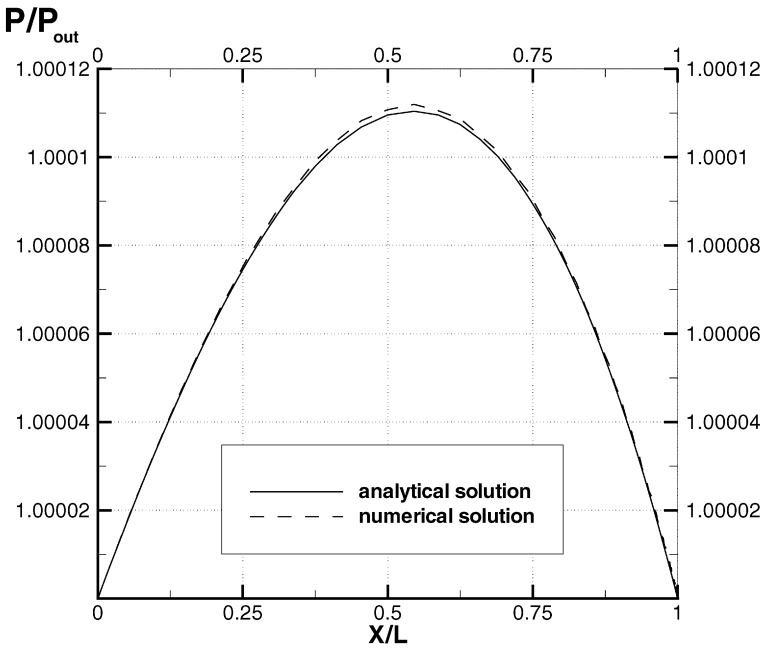

Fig. 2. Pressure profiles for helium flow, $Kn_{\text{out}} = 0.036$. The solid curve is the analytical solution, the dashed line represents the numerical solution.

Moreover, as it is well known, the BGK kinetic equation gives incorrect value of the Prandtl number, so this model cannot describe correctly the isothermal and non-isothermal flows simultaneously. Thus, the results obtained from BGK modelling [1] are not suitable for our case.

Therefore, we have compared our results with the results obtained in [2], where the kinetic approach is used and where the mass flow rates due to the pressure gradient and the temperature gradient are deduced separately from the solution of the S-model kinetic equation. Multiplying each mass flow rate by the corresponding gradient one obtains the global mass flow rate. But in the problem under consideration the pressure gradient *is* not known *a priori*. So, it is necessary to solve iteratively the differential equation for the pressure, where the global mass flow rate appears as a parameter.

The mass flow rates through the channel calculated numerically and analytically are compared in Tables 3–5 for the different flow conditions. The mass flow rate is calculated *for a* rectangular cross section with a width $w = 200$ μm. The analytical and numerical values of mass flow rate coincide practically for the small Knudsen numbers (see Tables 3 and 4) and start to differ *by* ∼3% for a Knudsen number *larger* than 0.25 (see Table 5).

The comparison with the results obtained in [2] applying the S-model kinetic equation are also carried out. There is a very good agreement between two approaches for the small Knudsen number and the maximal difference is of order of 15% for Knudsen number ∼0.25, see Tables 3–5. It is necessary to note at this point that [2] models the collision integral in the Boltzmann equation using the linearized S-model which gives a correct Prandtl number, but which is valid only for monatomic gases.

The non-linear pressure profiles (Eqs. (66) and (71)) along the streamwise direction are presented in Fig. 2 (helium flow, see Table 3). The transversal profiles of the streamwise velocity (Eq. (69)), for the flow conditions of Table 3, are shown in Fig. 3. It is interesting to note that in the first half of the channel the maximum of the velocity is found on the wall and the *pressure increases with x in the streamwise direction*, while in the second part the maximal velocity is on the axis, and the velocity profile has a typical form similar to the Poiseuille profile and the gas pressure decreases along the streamwise direction. Moreover the corresponding transversal temperature derivative profiles (Eq. (81)), opposite to the transversal heat flux, are shown in Fig. 4.

The influence of the temperature gradient along the wall is studied in the second series of calculations. The mass flow rate increases with the streamwise temperature gradients (see Table 4). Fig. 5 shows the streamwise velocity on the axis (obtained from Eq. (69) when $\tilde{y} = 0$) for three different values of this temperature gradient. The outlet

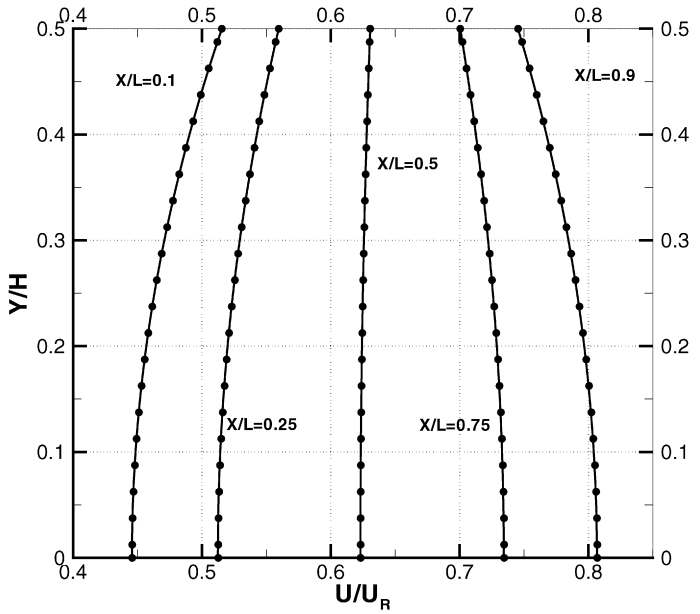

Fig. 3. Velocity profiles for helium flow in various sections of the channel, $Kn_{\text{out}} = 0.036$. The solid curve is the analytical solution, the circles represent the numerical solution.

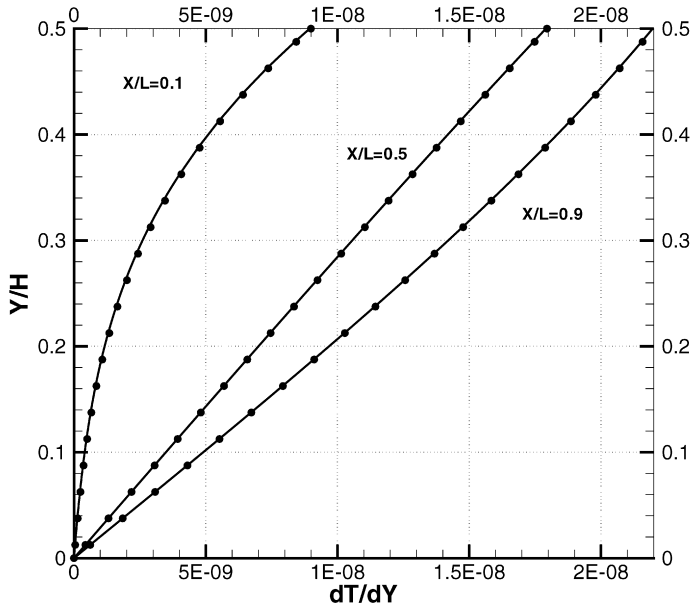

Fig. 4. Transversal temperature derivative profiles for the helium flow in various sections of the channel, $Kn_{\text{out}} = 0.036$. The solid curve is the analytical solution, the circles represent the numerical solution.

Knudsen number increases here only due to the temperature increase in the outlet reservoir since the pressure in the reservoir remains the same.

The influence of the reservoir pressures (i.e. of the Knudsen number, since the temperature difference remains the same when the pressure changes) is studied in a third series of calculations. It is to note that the dimensional mass flow rate depends weakly on the reservoir pressure for the pressure range under consideration (see Table 5), which is not surprising if considering analytical expressions (76) and (77). The influence of the Knudsen number on the pressure distribution is shown in Fig. 6. The pressure inside the channel increases when the Knudsen number increases. Figs. 7

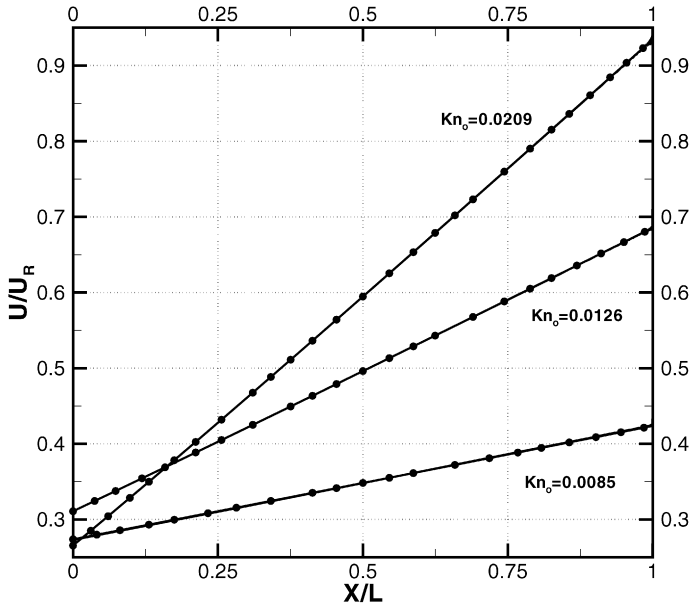

Fig. 5. Streamwise velocity along the axis for the nitrogen flow for the different temperature gradients. The solid curve is the analytical solution, the circles represent the numerical solution.

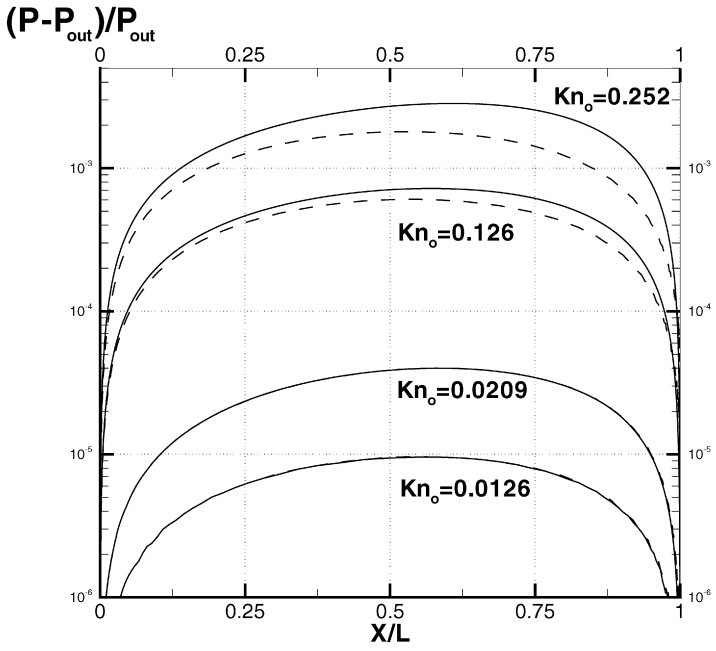

Fig. 6. Pressure profiles in nitrogen flows for different outlet Knudsen numbers. The solid curve is the analytical solution, the dashed line represents the numerical solution.

and 8 present the streamwise velocity distribution along the y axis in half of the micro channel for different Knudsen numbers, in two sections $x/L = 0.25$ and $x/L = 0.75$. All the velocities are here normalized with the local averaged velocity, namely:

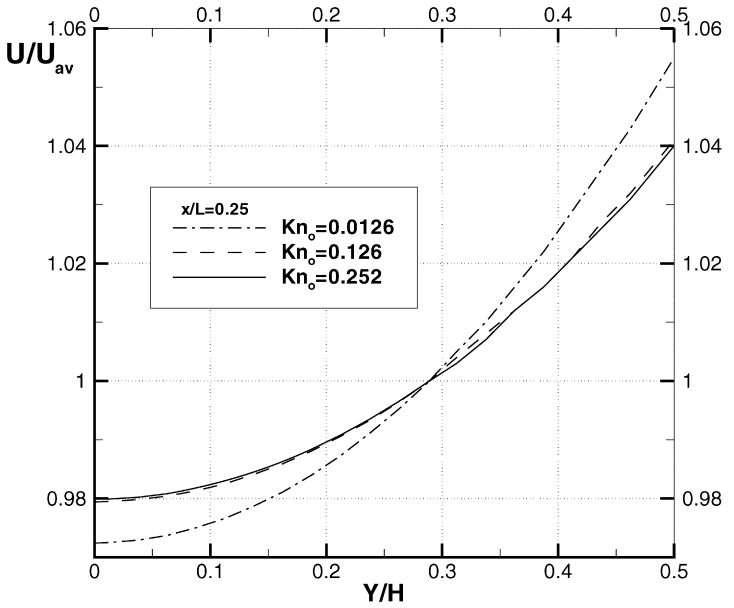

Fig. 7. Transversal velocity profiles in nitrogen flow for different Knudsen numbers at section $x/L = 0.25$.

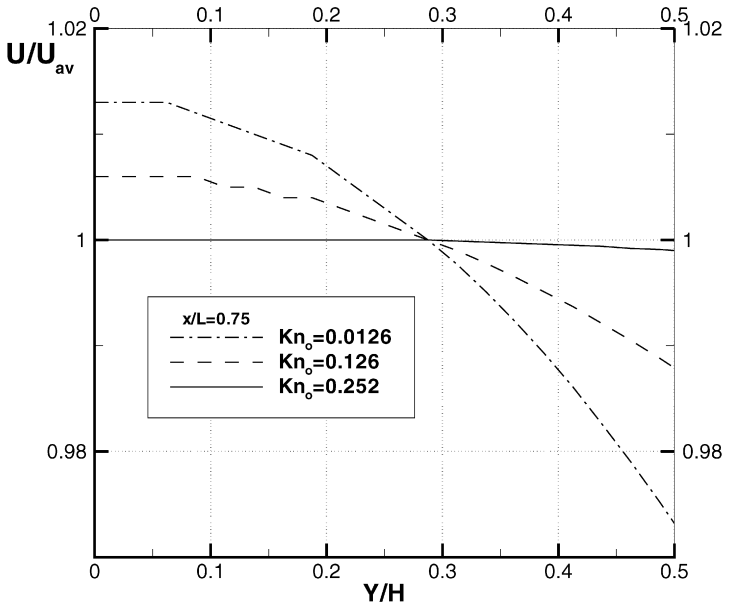

Fig. 8. Transversal velocity profiles in nitrogen flows for different Knudsen numbers at section $x/L = 0.75$.

$$\bar{u}(x) = \frac{2}{H} \int_0^{H/2} u(x, y)\, dy.$$

As was mentioned above, we can see that the velocity profiles have their maximal values at the wall in the first part of the channel (see Fig. 7) and on the channel axis in the second part of the channel (see Fig. 8). When the Knudsen number increases the profiles become smoother and finally quasi-uniform.

Generally, it is clear, from the different Figs. 2–6, that the analytical and numerical profiles are in very good agreement.

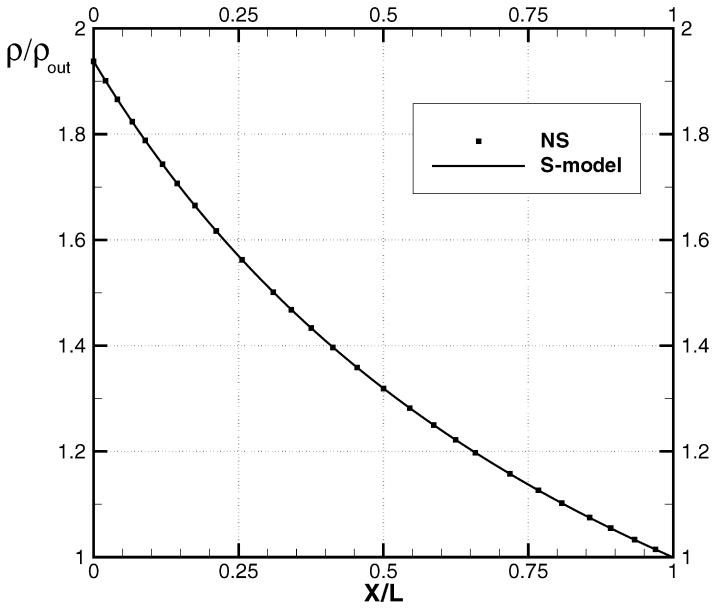

Fig. 9. Density profiles in helium flow, $Kn_{\text{out}} = 0.036$. The solid curve is the solution of the S-model kinetic equation, the squares represent the analytical solution.

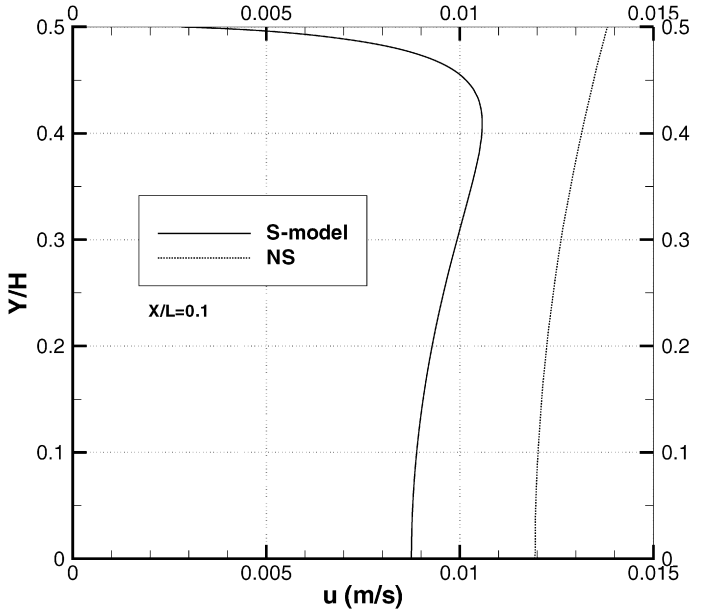

Fig. 10. Velocity profiles in helium flow, for $Kn_{\text{out}} = 0.036$. The solid curve is the solution of the S-model kinetic equation, the dashed line represents the analytical solution.

The comparison of the analytical profiles obtained with the results of the kinetic approach used in [2,15] are presented in Figs. 9–12 for the case of the helium flow. The density distributions given by two approaches are presented in Fig. 9 and coincide. The transversal velocity profiles in the different sections of the channel are presented in Figs. 10–12. The shape of the curves is the same for $\sim 80\%$ of the half section, but near the wall the profiles are different. This difference appears partially due to the Knudsen layer effects near the wall. Of course, the continuum approach overestimates the velocity near the wall and underestimates it in the center. But the Knudsen number considered here ($Kn = 0.036$) is rather small. In such moderate rarefied conditions, it is expected that the Knudsen layer

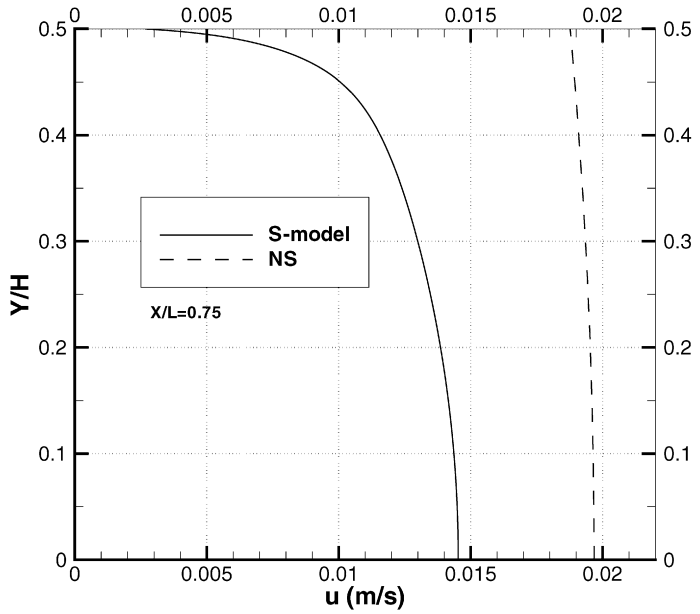

Fig. 11. Velocity profiles in helium flow, for $Kn_{\text{out}} = 0.036$. The solid curve is the solution of the S-model kinetic equation, the dashed line represents the analytical solution.

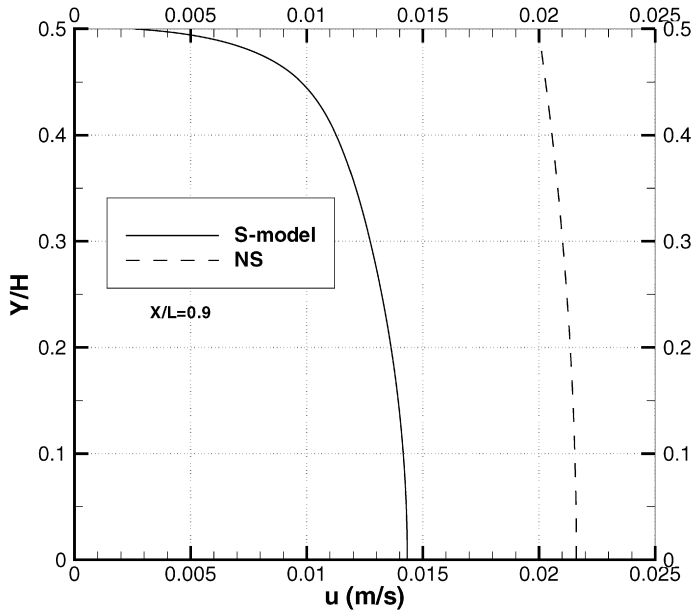

Fig. 12. Velocity profiles in helium flow, $Kn_{\text{out}} = 0.036$. The solid curve is the solution of the S-model kinetic equation, the dashed line represents the analytical solution.

effects may be conveniently taken into account using slip velocity and temperature jump boundary conditions, as we did. Moreover, this discrepancy between the two approaches does not increase when the Knudsen number increases up to 0.07, and does not diminish when the Knudsen decreases under 0.03. Therefore, to clarify this intriguing question and to improve the agreement between the results we will investigate toward two directions: first, an evaluation of the kinetic method precision, possibly small, if calculating the pressure (and thus velocity) profiles when the gradient vanishes, as in our case; then an extension of the continuum approach taking into account the second order effects.

Table 6
Driver gradients of the flows for the same mass flow rates. $\frac{T_{out}-T_{in}}{T_{out}}$ represents the quasi-isobar temperature gradient, $\frac{p_{out}-p_{in}}{p_{out}}$ the isothermal pressure gradient

$Q \times 10^{-12}$ kg/s	T_{in} (K)	$\frac{T_{out}-T_{in}}{T_{out}}$	p_{out} (Pa)	$\frac{p_{out}-p_{in}}{p_{out}}$	Kn_{isoth}	Kn_{therm}
3.76	295	0.484	p_{atm}	0.002	0.017	0.036
3.60	295	0.484	$0.1\,p_{atm}$	0.07	0.17	0.36

In any way, as quoted in the introduction, since our mass flow rate results agree with all the approaches used to model the phenomenon (*including the kinetic approach*), we used here our analytical formulation in order to easily compare the physical conditions respectively required to obtain the same fixed mass flow rates values, using respectively two typical driven flows (namely isothermal and thermal creep). This comparison is presented in Table 6. This comparison may be used to *choose* a driver gas system in a micro device, taking also into account that, when possible, the thermal driving presents a basic *advantage*; allowing to avoid any expensive micro pump or any uneasy external driver gas.

12. Concluding remarks

We have focused our interest on the non-isothermal steady continuum approaches in slip regime (up to Knudsen numbers close to 0.25) using the Navier Stokes equations. From this equation system, describing the case where the reservoir pressures are the same, we have derived a mass flow rate expression, the analytical profiles of pressures and velocities and the heat flux, using energy balance and small perturbation method. Globally in this Knudsen range our analytical profiles agree perfectly with the continuum "exact" numerical results and they agree reasonably with the results of the numerical solution of the S-model kinetic equation (if we disregards the velocity profiles in the closest wall neighboring where the discrepancies are more important). Such analytical expressions are original for compressible flows. They are obviously useful in the development of various micro devices using thermal creep effect to start and maintain gas motions in micro channels. Indeed explicit expressions of the gas physical quantities appear very easy to use; they especially minimize calculation time *required to find* the optimal values of sensitive parameters characteristic of any specific micro device.

Finally the main noticeable physical features appearing from the analytical description of the thermally creeping flows, presented here above, may be summarized as follows:

- the mass flow rate depends very weakly on the reservoir pressure and increases regularly with the streamwise temperature gradient.
- *the pressure profile along the streamwise direction is significantly non linear and presents a maximal value in a point* x_M *close to* 0.5. *The maximal dimensionless pressure difference* $\Delta\tilde{p}_M$ *is of second order according to the Knudsen number.*
- the curvature of the velocity transversal profiles changes at this x_M point. In the second part of the channel this curvature becomes similar to that of isothermal profiles; but the weight of the slip velocity remains everywhere more important than in the isothermal case.
- the non-dimensional transversal heat flux is a second order quantity according to the aspect ratio, as does the relative transversal temperature differences. These thermal parameters are not uniform over each a transverse section. In addition they very sensitively depend on the thermal slip coefficient σ_T.

Acknowledgements

The authors gratefully acknowledge the support given by the National Center of Scientific Research (CNRS), project number MI2F03-45 and International cooperation project with CNPq (Brazil) and especially Prof. F. Sharipov for helpful comments and discussions.

References

[1] T.S. Stvorik, H.S. Park, S.K. Loyalka, Thermal transpiration: A comparison of experiment and theory, J. Vac. Sci. Technol. 15 (6) (1978) 1844–1852.
[2] F. Sharipov, Non-isothermal gas flow through rectangular microchannels, J. Micromech. Microeng. 9 (1999) 394–401.
[3] T. Ohwada, Y. Sone, K. Aoki, Numerical analysis of the Poiseuille and thermal transpiration flows between two parallel plates on the basis of the Boltzmann equation for hard sphere molecules, Phys. Fluids A 1 (12) (1989) 2042–2049.
[4] Y. Sone, Kinetic Theory and Fluid Dynamics, Birkhäuser, 2002.
[5] G.E. Karniadakis, A. Beskok, Microflow: Fundamental and Simulations, Springer-Verlag, New York, 2002, p. 340.
[6] G.A. Bird, Molecular Gas Dynamics and the Direct Simulation of Gas Flows, Oxford University Press, New York, 1994.
[7] M.N. Kogan, Rarefied Gas Dynamics, Plenum Press, New York, 1969.
[8] C. Cercignani, Mathematical Methods in Kinetic Theory, second ed., Plenum, New York, 1990, (Chapter 4).
[9] F. Sharipov, Data on the velocity slip and temperature jump coefficients, in: L.J. Ernst, G.Q. Zhang, P. Rodgers, O. de Saint Leger (Eds.), Thermal and Mechanical Simulation and Experiments in Micro-Electronics and Micro-Systems, 5th Int. Conf. EuroSimE 2004, Shaker Publishing, 2004, pp. 243–249.
[10] B.T. Prodnov, A.N. Kulev, F.T. Tuchvetov, Thermal transpiration in a circular capillary with a small temperature difference, J. Fluid Mech. 88 (4) (1977) 609–622.
[11] M. Von Smoluchoski, Über Wärmeleitung in verdünnten Gasen, Annalen der Physik und Chemie (1898) 101–130.
[12] E. Kennard, Kinetic Theory of Gases, McGraw-Hill Book Co., Inc., New York, 1938.
[13] F. Sharipov, Application of the Cercignani–Lampis scattering kernel to calculations of rarefied gas flows. II. Slip and jump coefficients, Eur. J. Mech. B Fluids 22 (2003) 133–143.
[14] S. Chapman, T.G. Cowling, The Mathematical Theory of Non-uniform Gases, third ed., Cambridge University Press, Cambridge, 1970.
[15] F. Sharipov, Private communication, 2005.